

20 **Abstract**

21 Despite decades of investigation into how antibiotics affect isolated bacteria, it
22 remains highly challenging to predict consequences for communities in complex
23 environments such as the human intestine. Interspecies interactions can impact
24 antibiotic activity through alterations to the extracellular environment that
25 change bacterial physiology. By measuring key metabolites and environmental
26 pH, we determined that metabolic cross-feeding among members of the fruit fly
27 gut microbiota drives changes in antibiotic sensitivity *in vitro*. Co-culturing of
28 *Lactobacillus plantarum* with *Acetobacter* species induced tolerance to rifampin.
29 Mechanistically, we found that acetobacters counter the acidification driven by *L.*
30 *plantarum* production of lactate, and that pH shifts during stationary phase were
31 sufficient to drive rifampin tolerance in *L. plantarum* monocultures. The key
32 *Lactobacillus* physiological parameter related to tolerance was a reduction in lag
33 time exiting stationary phase, opposite to a previously identified mode of
34 tolerance to ampicillin in *E. coli*. *Lactobacillus* tolerance to erythromycin also
35 depended on growth status and pH, suggesting that our findings generalize to
36 other antibiotics. Finally, tolerance of *L. plantarum* to rifampin varied spatially
37 across the fruit fly gut. This mechanistic understanding of the coupling among
38 interspecies interactions, environmental pH, and antibiotic tolerance enables

- 39 future predictions of growth and the effects of antibiotics in more complex
40 communities and within hosts.

41 **Introduction**

42 Decades of investigations have described detailed and precise molecular
43 mechanisms of antibiotic action in model organisms. Yet, our current
44 understanding is biased by a narrow set of standardized laboratory conditions; a
45 recent study reported that resistance of *Escherichia coli* to the beta-lactam
46 mecillinam is rarer in clinical isolates than in the laboratory and involves distinct
47 genetic loci¹. Unlike in laboratory monocultures, the vast majority of bacteria live
48 in diverse communities such as the human gut microbiota. Antibiotics impact
49 gut communities in many ways, ranging from the loss of diversity^{2,3} to the
50 evolution of multidrug-resistant gut pathogens⁴. Hence, there is a pressing need
51 for new frameworks that predict how antibiotics affect bacterial communities.

52

53 Bacteria can survive antibiotics through (i) resistance mutations, which
54 counteract the antibiotic mechanism; (ii) persistence, whereby a subset of the
55 bacterial population survives the antibiotic by becoming metabolically dormant;
56 or (iii) tolerance, whereby the entire population enters an altered physiological
57 state that is not susceptible to the antibiotic⁵. Members of multispecies
58 communities, such as biofilms and models of urinary tract infections, can display
59 altered sensitivity to antibiotics⁶⁻⁹. A few studies have delved into the molecular
60 mechanisms behind cross-species antibiotic protection and sensitization. For

61 example, the exoproducts of *Pseudomonas aeruginosa* affect the survival of
62 *Staphylococcus aureus* through changes in antibiotic uptake, cell-wall integrity,
63 and intracellular ATP pools¹⁰. In synthetic communities, intracellular antibiotic
64 degradation affords cross-species protection against chloramphenicol¹¹.
65 Additionally, metabolic dependencies within synthetic communities can lower
66 the viability of bacteria when antibiotics eliminate providers of essential
67 metabolites, leading to an apparent change in the minimum inhibitory
68 concentration (MIC) of the dependent species⁹. However, we still lack
69 understanding of how contextual metabolic interactions between bacteria affect
70 the physiological processes targeted by antibiotics and the resulting balance
71 between growth inhibition (bacteriostatic activity) and death (bactericidal
72 activity).

73

74 Characterizing the impact of metabolic interactions on antibiotic susceptibility
75 requires functional understanding of how bacterial species interact during
76 normal growth. Interspecies interactions can occur through specific mechanisms
77 within members of a community (e.g. cross-feeding or competition for specific
78 resources), or through global environmental variables modified by bacterial
79 activity. An example of the latter is pH, which has recently been shown to drive

80 community dynamics in a highly defined laboratory system of decomposition
81 bacteria¹².

82

83 While synthetic communities afford the opportunity to design and to tune
84 bacterial interactions, it is unclear whether findings are relevant to natural
85 communities. The stably associated gut microbiota of *Drosophila melanogaster* fruit
86 flies constitutes a naturally simple model community for determining how
87 metabolic interactions between species affect growth, physiology, and the action
88 of antibiotics¹³. This community consists of ~5 species predominantly from the
89 *Lactobacillus* and *Acetobacter* genera¹⁴ (Fig. 1a). Lactobacilli produce lactic acid¹⁵,
90 while acetobacters are acetic acid bacteria that are distinguished by their ability
91 to oxidize lactate to carbon dioxide and water¹⁶. Short chain fatty acids, such as
92 lactate, decrease the pH of natural fermentations and may constitute a
93 mechanism through which pH plays a prominent role in community dynamics.
94 The naturally low number of species in *Drosophila* gut microbiota and its
95 compositional modularity (lactobacilli versus acetobacters) enable systematic
96 dissection of microbial interactions.

97

98 In the current study, we interrogated how interspecies interactions affect growth
99 and antibiotic susceptibilities. We used high-throughput assays to measure these

100 parameters in monocultures versus co-cultures and inside fly guts. *Lactobacillus*
101 *plantarum* (*Lp*) exhibited antibiotic tolerance (delay in death⁵ by ~12 h) in the
102 presence of acetobacters. Lactate accumulation by *Lp* in monocultures acidified
103 the media, inhibiting growth during stationary phase. *Acetobacter*-mediated
104 lactate consumption released this inhibition by increasing pH, leading to a
105 shorter *Lp* lag while exiting stationary phase. This reduced lag exiting stationary
106 phase corresponded with the antibiotic tolerance of *Lp* that we observed. We
107 determined that changes in pH elicited by *Acetobacter* activity are sufficient to
108 modulate tolerance of *Lp* to both rifampin and erythromycin. Finally, *ex vivo*
109 experiments revealed that antibiotic tolerance differs in distinct compartments of
110 the host gastrointestinal tract. Taken together, our findings indicate that simple
111 changes to the environment can drive complex behaviors within bacterial
112 communities.
113

114 **Results**

115

116 *Interspecies interactions induce tolerance to rifampin*

117 To determine the composition of the gut microbiota in our laboratory fruit flies,
118 we performed deep sequencing of 16S rRNA V4 amplicons from 18 individual
119 dissected guts (Methods). We identified five species belonging to seven unique
120 operational taxonomic units (OTUs) by clustering the sequences at 99% identity:
121 *L. plantarum* (*Lp*), *L. brevis* (*Lb*), *Acetobacter pasteurianus* (*Ap*), *A. tropicalis* (*At*), and
122 *A. aceti* (*Aa*) (Fig. 1a). We then isolated the species in culture and determined the
123 antibiotic sensitivities of the four major fly gut inhabitants (*Lp*, *Lb*, *Ap* and *At*; Fig.
124 1a) *in vitro* using isolates of these species (Table S1) grown in Man, Rogosa, and
125 Sharpe (MRS) medium. We tested 10 antibiotics representing a wide variety of
126 classes using plate-based growth assays (Methods). For many drugs, some of the
127 fly gut species were resistant (detectable growth) at least up to the highest
128 concentrations tested. Rifampin was the only drug for which all four species
129 exhibited sensitivity (Table S2) and it is bactericidal¹⁷, hence there is the
130 opportunity to study survival as well as sensitivity.

131

132 We noted from growth curves in the absence of drug that *Lb* grew significantly
133 more slowly than *Lp* ($0.60 \pm 0.054 \text{ h}^{-1}$ vs. $0.64 \pm 0.001 \text{ h}^{-1}$ for *Lp*, $P = 5.5 \times 10^{-3}$, $n = 16$,

134 Fig. S1) and had a much longer lag phase than *Lp* (6.55 ± 0.16 h vs. 1.92 ± 0.08 h
135 for *Lp*, $P = 1.8 \times 10^{-39}$, $n = 16$, Fig. S1). Thus, we focused on *Lp* and its interactions
136 with the *Acetobacter* species, particularly *Ap*, which is more abundant in the fly
137 gut than the other acetobacters (Fig. 1a).

138

139 We grew *Lp* and *Ap* separately for 48 h in test tubes, combined them in test tubes
140 at an optical density at 600 nm (henceforth OD) of 0.02 each, and co-cultured
141 them in MRS for 48 h. We then diluted this co-culture and 48-h monocultures of
142 *Lp* and *Ap* into fresh MRS at $\sim 5 \times 10^5$ colony-forming units/mL (CFU/mL) in 96-
143 well plates with various concentrations of rifampin and measured growth over
144 48 h. The MIC of the co-culture was similar to that of *Lp* alone ($2.5 \mu\text{g/mL}$, Fig.
145 S2a). To determine whether the co-culture still contained both species, we
146 measured the percentage of survival and the fraction of each species at various
147 rifampin concentrations by taking advantage of the fact that *Lp* and the
148 acetobacters have distinct colony morphologies and colors on MRS and MYPL
149 plates (Table S1). We measured *Lp* CFUs on MRS and *Ap* CFUs on MYPL because
150 *Lp* and *Ap* grow more quickly on MRS and MYPL, respectively. In the co-culture,
151 *Ap* died off at a similar concentration of rifampin as during growth in a
152 monoculture ($1.25 \mu\text{g/mL}$, Fig. S2b). For *Lp*, the MIC was the same in co-culture
153 as in monoculture ($1.25 \mu\text{g/mL}$, Fig. 1b), but at concentrations above the MIC,

154 significantly more *Lp* cells survived in co-culture than in monoculture (Fig. 1b).

155 This effect could not be explained by small differences in the initial inoculum, as
156 increasing cell densities up to 100-fold did not change the MIC or survival of *Lp*
157 in monoculture (Fig. S2c,d). Because of the change in *Lp* survival, we focused
158 herein on this phenotype.

159

160 To determine whether *Lp*'s increased survival was specific to co-culturing with
161 *Ap*, we co-cultured *Lp* with each of the acetobacters, including a wild fly isolate
162 of *A. indonesiensis* (*Ai*), and lab fly isolates of *A. orientalis* (*Ao*) and *Aa*, the fifth
163 major component of the microbiota of our flies (Fig. 1a). We then diluted each co-
164 culture to an initial *Lp* cell density of $\sim 5 \times 10^5$ CFU/mL into fresh MRS with 20
165 $\mu\text{g/mL}$ rifampin (16X MIC) and let the cells grow for 24 h. Co-culturing with any
166 of the acetobacters increased survival by approximately one order of magnitude
167 (Fig. 1c). To determine whether this increased survival requires co-culturing
168 prior to rifampin treatment (rather than the presence of the acetobacters being
169 sufficient), we grew *Lp* and *Ap* separately for 48 h and mixed and diluted them at
170 the time of addition of 20 $\mu\text{g/mL}$ rifampin. After 24 h of growth, the number of
171 CFU/mL was significantly lower in mixed culture than in co-culture (Fig. 1d),
172 indicating a history dependence to increased survival.

173

174 To determine whether co-culturing slows killing by the drug, we examined the
175 survival of *Lp* over time at a high drug concentration (50 $\mu\text{g}/\text{mL}$, 40X MIC).
176 Similar to the experiments above, we compared *Lp* CFU/mL in a monoculture
177 with that in a co-culture with *Ap*. In monoculture, *Lp* rapidly died, with CFU/mL
178 becoming undetectable within 18 h; in contrast, *Lp* survived >30 h after co-
179 culturing (Fig. 1e). This increased time to death of *Lp* as a bulk population, and
180 unchanged MIC, together indicate that co-culturing *Lp* with *Ap* induces tolerance
181 of *Lp* to rifampin⁵.

182

183 *Co-culturing leads to growth of Lp in stationary phase*

184 Our finding that co-culturing *Lp* with acetobacters affects antibiotic tolerance
185 (Fig. 1c,e) prompted us to investigate the environmental factors that cause this
186 phenotype. We first inquired whether the total amount of growth of the co-
187 culture was larger or smaller than expected from the yield of the monocultures.
188 We grew *Lp* and each of the acetobacters separately for 48 h, diluted the
189 monocultures to OD = 0.04, combined the *Lp* monoculture 1:1 with each
190 *Acetobacter* monoculture, and grew the co-cultures for 48 h in test tubes. In bulk
191 measurements, the *Lp*-*Ap* co-culture showed a significant synergistic effect
192 (Supplementary Text, Fig. S3a). We then determined the total carrying capacity
193 of each of the species in the co-cultures grown in test tubes by counting CFUs.

194 We determined that the *Lp* CFU/mL values for 48-h co-cultures with *Ap*, *At*, and
195 *Ai* were higher than the *Lp* CFU/mL values in monoculture (Fig. 2a). Co-cultures
196 with *Ap* showed the strongest effect; *Aa* and *Ao* did not significantly increase *Lp*
197 CFU/mL (Fig. 2a). All acetobacters except for *Ap* reached lower CFU/mL in co-
198 cultures with *Lp* than in monocultures (Fig. S3b). Thus, *Lp* has a strong positive
199 interaction with *Ap*, and negative or neutral interactions with the rest of the
200 acetobacters (Supplementary Text, Fig. S3c).

201

202 To determine when the additional growth took place, we monitored CFU/mL
203 values for *Lp* and *Ap* in co-culture throughout a 48-h time course starting from an
204 initial combined cell density of $\sim 5 \times 10^5$ CFU/mL. Initially, *Lp* accounted for the
205 bulk of the growth in the co-culture (Fig. 2b). Interestingly, *Ap* in liquid
206 monoculture showed little to no growth in most replicates after 40 h (Fig. 2b); by
207 contrast, in liquid co-culture *Ap* started to grow after ~ 20 h and reached
208 saturation by ~ 40 h (Fig. 2b), indicating that *Ap* also benefited from growth as a
209 co-culture. This benefit likely stemmed from a reduction in *Ap* cell death during
210 lag phase (Supplementary Text, Fig. S4). Thus, a mutualism exists between *Lp*
211 and *Ap* driven by growth during and exiting from stationary phase.

212

213 *Lactate metabolism leads to changes in pH in stationary phase co-cultures*

214 Interestingly, after 30 h, *Lp* displayed a significant (~2X) increase in CFU/mL in
215 the co-culture that did not occur in the monoculture (Fig. 2b), indicating that the
216 increase in final yield occurs late in stationary phase. We therefore hypothesized
217 that *Lp* has a common metabolic interaction with each of the acetobacters. An
218 obvious candidate is cross-feeding, since *Lp* produces lactate and the acetobacters
219 consume it. We measured lactate levels in the supernatants of *Lp* monocultures
220 and co-cultures of *Lp* with each of the acetobacters individually, after 48 h of
221 growth. As expected, the *Lp* monoculture accumulated L- and D-lactate to high
222 levels (>100 mM; Fig. 2c). All co-cultures had significantly lower concentrations
223 of both isomers than the monoculture (<2 mM, Fig. 2c). The *Lp-Ao* co-culture
224 harbored higher levels of L-lactate than any other co-culture and *Lp-Aa* had
225 higher concentration of L-lactate than the rest of the co-cultures (Fig. 2c). *Lp-Ap*,
226 *Lp-Ao*, and *Lp-Aa* co-cultures all accumulated lactate (>10 mM) at 20 h (Fig. S5a).
227 Taken together, these data suggest that *Lp* metabolism leads to an initial
228 accumulation of lactate and that the acetobacters consume it, although *Aa* and *Ao*
229 are less efficient at consuming L-lactate than the other species.

230

231 Since lactate is a short-chain fatty acid with a pK_a of 3.86, we suspected that
232 lactate production would affect the pH of the culture. We first monitored the pH
233 dynamics of monocultures of *Lp* and of each *Acetobacter* using the pH-sensitive

234 fluorophore 2',7-bis-(2-carboxyethyl)-5-(and-6)-carboxyfluorescein (BCECF)¹⁸. In
235 the *Lp* monoculture, pH decreased from pH=6.75 to below 4 during growth (Fig.
236 2d); more precisely, we measured a final supernatant pH=3.77 using a pH meter
237 (Fig. S5a). We measured pH over time in *Acetobacter* monocultures using BCECF.
238 For all acetobacters except *Ap*, the medium first acidified down to pH~5, and
239 then increased back to pH=6-7 (Fig. 2d).

240

241 To test whether acetobacters reverse the pH decrease due to the accumulation of
242 lactate produced by *Lp*, we measured the pH of co-cultures over time using
243 BCECF. Co-cultures with *Ap*, *At*, and *Ai* followed similar trajectories in which the
244 pH followed that of the *Lp* monoculture for the first 20 h, after which the pH
245 increased up to a final value of ~7 (Fig. 2f). The *Lp-Aa* co-culture experienced a
246 ~10-h delay in the pH increase, while the co-culture with *Ao* showed only a slight
247 pH increase by 48 h (Fig. 2f). The slight pH increase in *Ao* co-culture is consistent
248 with lower L-lactate consumption by this species (Fig. 2c). Using a pH meter for
249 validation, we measured final pH values of 5.9, 5.8, 4.6, 5.4, and 4.8 in co-cultures
250 with *Ap*, *At*, *Ao*, *Ai*, and *Aa*, respectively (Fig. S5b). Thus, lactate metabolism
251 dictates dramatic shifts in environmental pH that are related to physiological
252 changes in antibiotic tolerance (Fig. 1c).

253

254 Given the strong acidification of the medium in *Lp* monoculture but not in co-
255 culture (Fig. 2d), we hypothesized that intracellular pH decreases in monoculture
256 and increases in co-culture. To measure intracellular pH, we transformed our *Lp*
257 strain with a plasmid expressing pHluorin (a GFP variant that acts as a
258 ratiometric pH sensor¹⁹) under the control of a strong constitutive promoter²⁰.
259 The two absorbance peaks, which we measured at 405 and 475 nm, are sensitive
260 to pH and the ratio of the emission (at 509 nm) at these two excitation
261 wavelengths can be used to estimate intracellular pH. We grew this strain in
262 monoculture and in co-culture with *Ap* and measured fluorescence over time in a
263 plate reader. Because of the high autofluorescence of the medium at 405 nm (data
264 not shown), we could only track changes in fluorescence at an excitation
265 wavelength of 475 nm. We observed an initial increase in signal as the *Lp* cells
266 started to proliferate (Fig. S6a). After the cultures saturated ($t \sim 20$ h), we detected
267 a decrease in the signal down to the levels of medium autofluorescence in the
268 monoculture (Fig. S6a). In the co-culture, where the extracellular pH is raised by
269 the metabolic activity of *Ap*, fluorescence did not decrease over time (Fig. S6a),
270 suggesting that intracellular pH decreases in a time-dependent manner in
271 monoculture but not in co-culture.

272

273 To verify that the decrease in fluorescence in monoculture was due to a drop in
274 intracellular pH, as opposed to a decrease in protein synthesis, we sampled cells
275 after 48 h of growth, centrifuged them, resuspended them in PBS in order to
276 measure pHluorin signal at both its excitation wavelengths, and measured
277 fluorescence within 1 minute of resuspension. The ratio of the signal from
278 pHluorin at its two excitation wavelengths was significantly higher in co-culture
279 (Fig. S6b). Taken together, these data indicate that the intracellular pH of *Lp* cells
280 is significantly lower in monoculture than in co-culture with acetobacters.

281

282 *Low pH inhibits the growth of Lp and extends lag phase*

283 Since *Ap* growth causes a large increase in the extracellular pH of an *Lp-Ap* co-
284 culture, we sought to determine the dependence of *Lp* growth on pH. We diluted
285 a 48-h culture of *Lp* cells grown in MRS at starting pH=6.75, to a starting OD=0.02
286 in MRS adjusted to starting pH ranging from 3 to 8 (Methods). We then
287 measured growth and BCECF fluorescence in a plate reader (Fig. S7a,b). For
288 lower starting pH values, the carrying capacity was lower (Fig. 3a) and varied
289 over a large OD range from <0.02 to >2. For all starting pH values, *Lp* cells
290 reduced the pH to a common final value of ~3.7 (Fig. 3a). The bulk growth rate
291 approached zero (Fig. 3b) as the pH approached its final value, explaining the

292 differences in yield. Interestingly, the maximum growth rate was also pH-
293 dependent (Fig. 3c), with the highest growth rate at starting pH=7.

294

295 Given these findings, we hypothesized that the inhibition of growth in stationary
296 phase of an *Lp* monoculture is due to the decreased intracellular and extracellular
297 pH, and that *Ap* releases *Lp*'s growth inhibition by raising intracellular and
298 extracellular pH. To test this hypothesis, we inoculated a 48-h culture of *Lp* to an
299 initial OD=0.02 into the supernatant of a 48-h *Lp* culture at pH=3.77 or set to
300 pH=7. We observed substantially more growth (~20-fold increase) of the bulk
301 culture in supernatant raised to pH=7, while no growth took place starting from
302 pH=3.77 (Fig. 3d). As expected, the maximal growth rate was lower than in fresh
303 MRS due to the partial depletion of nutrients (Fig. 3d); addition of glucose to the
304 conditioned medium supported faster growth, but only starting from neutral pH
305 (Fig. S7c). We also hypothesized that the accumulation of lactate by *Lp* would
306 allow growth of *Ap* in *Lp*-conditioned medium even at low starting pH. When
307 we diluted a saturated *Ap* culture into *Lp*-conditioned medium generated as
308 above, *Ap* grew to similar levels as in fresh MRS (Fig. S7d).

309

310 These findings suggested that the effects of *Ap* in co-culture on *Lp* growth might
311 be due primarily to the pH changes that *Ap* initiates because of the ability of

312 acetobacters to grow at low pH and to consume lactate. Thus, we first increased
313 the pH of an *Lp* monoculture to 7 after 30 h, when the pH increased most rapidly
314 in the *Lp*-*Ap* co-culture (Fig. 3e), and incubated cells for an additional 18 h. We
315 did not observe a significant increase in CFU/mL from this pH-adjusted culture
316 versus controls that simply grew for 48 h or were subjected to all washes
317 required for pH adjustment and then returned to the same supernatant (Fig. S7e).
318 We then assessed if increasing the pH at 30 h resulted in a decrease in the
319 duration of lag phase by diluting the monoculture to OD=0.0375 into fresh MRS
320 after an additional 18 h of growth. The lag phase was shorter in the pH-adjusted
321 culture than control bulk cultures (Fig. 3e). Thus, pH is a driver of the growth
322 advantages of *Lp* in lag phase.

323

324 *Co-culturing Lp with acetobacters reduces lag time*

325 Canonical antibiotic tolerance in *E. coli* results from a decrease in growth rate or
326 an increase in lag phase that protects cells through metabolic inactivity⁵. To
327 measure growth rate and lag phase, we co-cultured *Lp* with each of the
328 acetobacters individually for 48 h, diluted the culture to a common OD of 0.0375,
329 and monitored growth in a plate reader. The maximum growth rate was the
330 same for the *Lp* monoculture and co-cultures with *Ap*, *At*, and *Ai*, and slightly
331 higher for co-cultures with *Ao* and *Aa* (Fig. S8). We previously observed for *Lp*

332 monocultures when shifting the pH that the stimulation of growth in stationary
333 phase was connected with tolerance (Fig. 3e), opposite to that of *E. coli* tolerance
334 to ampicillin⁵. In agreement with these data, there was a significant decrease in
335 bulk lag time for all of the *Acetobacter* co-cultures (Fig. 4a,b). *Ap*, *At*, and *Ai* co-
336 cultures had the largest lag decreases. The *Aa* and *Ao* co-cultures had a smaller,
337 although still significant, decrease (Fig. 4a,b); interestingly, *Aa* and *Ao* were also
338 less efficient at consuming lactate than the other *Acetobacter* species (Fig. 2c).
339 These data indicate that interspecies interactions can change the physiology of
340 the community, and that differences across the acetobacters constitute an
341 opportunity to probe the underlying cause of the lag phenotype.

342

343 As with *Lp* tolerance to antibiotics (Fig. 1b), the shortened lag phase of the *Lp-Ap*
344 co-culture was history dependent. When we mixed 48-h cultures of *Lp* and *Ap* to
345 a combined initial OD of 0.0375 in the absence of antibiotics, the resulting bulk
346 culture had the same lag time as an *Lp* monoculture (Fig. 4c,d). To determine
347 which of the two species was responsible for the decrease in lag, we diluted a 48-
348 h co-culture of *Lp* and *Ap* 1:200, spotted 2 μ L onto a 1% agarose + MRS pad, and
349 performed time-lapse microscopy (Methods) to monitor the initiation of growth
350 at the single-cell level (Fig. 4e). *Lp* and *Ap* are clearly distinguishable based on
351 morphology (Fig. S9): *Lp* cells are longer ($2.46 \pm 0.78 \mu\text{m}$ vs. $1.66 \pm 0.38 \mu\text{m}$) and

352 thinner ($0.72 \pm 0.12 \mu\text{m}$ vs. $0.90 \pm 0.09 \mu\text{m}$) than *Ap* cells. Therefore, we used the
353 aspect ratio (length/width; 3.41 ± 0.91 for *Lp* and 1.87 ± 0.46 for *Ap*) to distinguish
354 single cells from each species in co-culture. We validated this strategy on co-
355 cultures of fluorescently tagged strains of the same two species and observed a
356 10% error rate in classification (Fig. S9d-f). In co-culture, most *Lp* cells were
357 observed to have grown by 1 h after spotting, but in *Lp* monoculture, few cells
358 were growing even after 2 h (Fig. 4e,f). *Ap* cells did not grow during the time of
359 imaging (Fig. 4f), indicating that the reduced lag time was due to *Lp*'s growth, in
360 agreement with CFU/mL measurements (Fig. 2b).

361

362 *Growth status and pH are drivers of antibiotic tolerance*

363 Since pH changes shortened lag phase (Fig. 3e), and since changes in lag time
364 were related to antibiotic tolerance (Fig. 1,4), we tested whether shortening lag
365 phase was sufficient to induce tolerance. Lag phase can be manipulated by
366 increasing time in starvation²¹. To determine the relationship between time spent
367 in stationary phase and lag time in *Lp*, we diluted a 48-h monoculture to a
368 starting OD=0.02 in fresh medium and grew it for varying amounts of time. We
369 then diluted these monocultures into fresh medium at OD=0.0375 and measured
370 bulk culture growth in a plate reader. Incubating the *Lp* monocultures for more

371 than 48 h resulted in a dramatic increase in the duration of lag phase, while
372 reducing the culturing time shortened lag phase (Fig. 5a).

373

374 Because lag phase in co-culture is slightly shorter than that of a 24-h monoculture
375 (Fig. 5a), we decided to match the lag time of a co-culture by growing a
376 monoculture for 20 h from an initial OD=0.02. We then measured *Lp* survival in
377 20 µg/mL rifampin after 24 h in cultures diluted from a 48-h-old or a 20-h-old
378 culture. Culturing for 20 h resulted in a significant increase in survival (Fig. 5b).

379 We next tested whether shortening lag phase by changing the pH in stationary
380 phase also yielded increased rifampin tolerance of *Lp* in co-culture. We increased
381 the pH of an *Lp* monoculture to 7 after 30 and 40 h, and grew cells for an
382 additional 18 h and 8 h, respectively. We then measured the change in CFU/mL
383 upon treatment with 50 µg/mL rifampin for 24 h. The upshift in pH at $t = 30$ h or
384 40 h resulted in increased tolerance relative to the unshifted monoculture (Fig.
385 5c). To test the extent to which changes in pH affect tolerance, we grew co-
386 cultures of *Lp* and *Ap* for a total of 48 h and decreased the pH to 3.7 at $t = 30$ h or
387 40 h. In both cases, the viability after 24 h of rifampin exposure was significantly
388 reduced relative to an untreated monoculture (Fig. 5d). Thus, pH can affect
389 tolerance both positively and negatively.

390

391 In co-culture with *Lp*, *Ap* raised the pH earlier than did *Aa*, while *Ao* only raised
392 the pH very slightly (Fig. 2d). We hypothesized that due to these distinct pH
393 dynamics, rifampin would also have different killing *Lp* dynamics in these co-
394 cultures. We grew co-cultures of these acetobacters with *Lp* as previously, and
395 then treated the co-cultures with 50 µg/mL rifampin. While all co-cultures had
396 extended survival relative to *Lp* monoculture, the killing dynamics of *Lp* were
397 indeed distinct, with *Aa* inducing the highest tolerance (Fig. 5e). To determine
398 the extent to which these dynamics can be explained by the time at which each
399 species raises the pH, we measured CFU/mL at various time points after
400 rifampin treatment for *Lp* monocultures grown for 48 h whose pH was raised to
401 pH 7 at $t = 30$ h or 40 h, mimicking the early and late increases in pH for *Ap* and
402 *Aa* co-cultures, respectively. The shift to pH 7 at 40 h induced higher rifampin
403 tolerance than the shift at 30 h (Fig. 5f), consistent with the increased tolerance of
404 the *Lp*-*Aa* co-culture (Fig. 5e). Moreover, shifting the pH to 4.5 at $t = 30$ h, to
405 mimic the slight increase caused by *Ao*, was also sufficient to increase tolerance
406 comparable to pH neutralization at $t = 30$ h (Fig. 5f), consistent with the similar
407 killing dynamics of the *Ap* and *Ao* co-cultures (Fig. 5e). All pH shifts induced
408 higher tolerance compared to control cultures that underwent the same protocol
409 but whose pH was maintained (Fig. 5f). Taken together, these experiments

410 establish that pH changes drive the tolerance of *Lp* to rifampin through changes
411 in the exit from stationary phase.

412

413 *Growth status and pH also drive tolerance to a ribosome-targeting antibiotic*

414 The robust relationships among changes in pH, lag time, and rifampin tolerance

415 prompted us to explore how changes in pH and lag time affect survival to other

416 antibiotics. We decided to use the ribosome-targeting macrolide erythromycin

417 because it is bactericidal and *Lp* is sensitive to it (Table S2). We treated *Lp*

418 monocultures grown for 20 h or 48 h with increasing concentrations of

419 erythromycin for 24 h at a starting cell density of $\sim 5 \times 10^5$ CFU/mL. In contrast to

420 our observations with rifampin (Fig. 5b), a 48-h *Lp* monoculture displayed

421 tolerance to erythromycin, while a 20-h culture did not (Fig. 5g). While both

422 cultures had the same MIC in erythromycin (0.078 μ g/mL, Fig. 5g), at

423 concentrations above the MIC, the 48-h culture showed no changes in CFU/mL

424 after 24 h of erythromycin treatment; the 20-h culture had a reduction of ~ 10 -fold

425 in CFU/mL (Fig. 5g). This result suggests that *Lp* cells diluted from a 48-h culture

426 are tolerant to erythromycin, opposite to the effect we observed with rifampin.

427

428 To further determine whether antibiotic tolerance underlies the survival of *Lp* to

429 erythromycin as well as to rifampin, we diluted 20- and 48-h cultures to a

430 starting density of $\sim 5 \times 10^5$ CFU/mL, exposed them to a high concentration of
431 erythromycin (2 μ g/mL, 25X MIC), and monitored CFU/mL over time. Cells from
432 a 20-h culture died significantly more rapidly than cells from a 48-h-old culture
433 (Fig. 5h), indicating that the differences in survival (Fig. 5g) are explained by
434 erythromycin tolerance. Further, increasing the pH of an *Lp* monoculture at 30 h
435 and then exposing it after an additional 18 h of growth to 2 μ g/mL erythromycin
436 in fresh medium had an increase in the rate of killing that was similar to that
437 achieved with a 20-h culture (Fig. 5h). These results highlight that the effects of
438 changing the growth status of a culture by different means are not limited to
439 rifampin and—as in the case of erythromycin—can be opposite.

440

441 *Growth state in the fruit fly gut determines antibiotic tolerance ex vivo*

442 Our *in vitro* observations connecting changes in pH to lag time and antibiotic
443 tolerance prompted us to examine whether these properties are also linked
444 within the fruit fly gut. This tract consists of a ~ 5 -mm-long tube divided into
445 three sections: foregut, midgut, and hindgut (Fig. 5i). The foregut includes an
446 accessory storage organ known as the crop. The contents of the crop are
447 delivered to the midgut through the proventriculus and transit through the
448 midgut to end in the hindgut, where they are expelled into the environment
449 through the rectum and the anus²². Specialized “copper” cells in the central

450 portion of the midgut keep the pH of this section low, akin to the stomach in
451 mammals²³. Bacteria are distributed along the *Drosophila* gastrointestinal tract; *Lp*
452 in particular can colonize all compartments with slight variations in its
453 distribution along the tract²⁴.

454

455 To examine whether variations along the fly gut impact *Lp* physiology, we
456 coarse-grained the digestive tract into the crop and the midgut and quantified
457 rifampin tolerance of *Lp* from these regions. We hypothesized that the different
458 functions of these regions – storage, or nutrient absorption and transit – lead to
459 differences in bacterial physiology. We colonized 5-7-day-old, female, germ-free
460 flies with *Lp* and left them for three days in sterile food to reach equilibrium
461 (Methods). We then dissected the flies and separated the crop from the midgut.
462 We pooled (i) dissected crops and (ii) dissected midguts in MRS to obtain a final
463 bacterial density of $\sim 5 \times 10^5$ CFU/mL. Crops had overall ~ 10 times less *Lp* than the
464 midgut (8,700 CFU/crop vs. 86,000 CFU/midgut). After homogenization, the
465 samples were exposed to 20 $\mu\text{g/mL}$ or 50 $\mu\text{g/mL}$ rifampin for 24 h. The MIC of
466 rifampin for these *ex vivo* samples was approximately the same as for *in vitro*
467 cultures (1.25 $\mu\text{g/mL}$). For cultures extracted from the crop, significantly more
468 cells survived than for cultures extracted from the midgut, with values
469 comparable to those of a co-culture with *Ap* and a monoculture, respectively (Fig.

470 5j). These results indicate that spatial heterogeneity in the host can lead to
471 differences in the duration of lag phase and antibiotic tolerance *ex vivo*.

472 **Discussion**

473 Our measurements of the growth behavior of the fly gut microbiota indicate that
474 interspecies interactions impact both the metabolism of a microbial community
475 and the effect of antibiotics on individual species. For fly gut commensals, the
476 pH-based mechanism underlying the tolerance of *Lp* induced by acetobacters is
477 intrinsically connected to the metabolic capacity of each species, and hence is
478 likely to be generally relevant *in vivo* to the resilience of this community under
479 perturbations. Moreover, these findings could have important implications for
480 human health, for example in the context of *Lactobacillus*-dominated vaginal
481 microbiotas²⁵, and their generality should be tested broadly in other contexts.

482

483 In this study, we observed a novel form of antibiotic tolerance. Tolerance has
484 been defined as increased time to killing²⁶, as opposed to resistance (a change in
485 the MIC), or persistence (the ability of a subpopulation of clonal bacteria to
486 survive high concentrations of antibiotic⁵). Tolerance to beta lactams such as
487 ampicillin has been observed in *E. coli* cultures that exhibit slow growth or a long
488 lag phase⁵, and *E. coli* mutants with longer lag phases can be selected through
489 experimental evolution to match the time of treatment^{27,28}. Based on these
490 previous studies, we were surprised to find the opposite effect with rifampin on
491 *Lp*: cultures with a shorter lag phase exhibited increased tolerance (Fig. 1,4).

492 Moreover, although tolerance to erythromycin was associated with a longer lag
493 phase (Fig. 3e, 5a,h), killing retardation was at least an order of magnitude longer
494 than the change in lag time (Fig. 5a,h), indicating that tolerance is not determined
495 by an elongation of lag phase alone, in contrast to the effects of ampicillin on *E.*
496 *coli*²⁷.

497

498 Several genetic factors that increase time to killing have been identified in *E. coli*,
499 including toxin-antitoxin modules such as *hipBA*²⁹ that induce the stringent
500 response and thus cause transient growth arrest. In *Lp* co-culture with
501 acetobacters, metabolic interactions alter the physiological state of *Lp* during late
502 stationary phase by changing the environmental pH (Fig. 2). The stringent
503 response is required to survive acid shock in *Helicobacter pylori*³⁰ but not in
504 *Enterococcus faecalis*³¹, which is in the same order as *Lp*. In the case of *Lp*, whether
505 the stringent response could be a major factor in the increased tolerance to
506 rifampin is unclear due to the surprising connection with decreased lag (not to
507 mention the opposite behavior with erythromycin).

508

509 The pH in stationary phase can affect many factors, such as the chemistry of
510 extracellular metabolites and macromolecules as well as the surface of the cell³².
511 Importantly, our assays of antibiotic sensitivities were all performed at a starting

512 pH of 7. Nonetheless, shifts in extracellular pH can lead to buffered drops in
513 cytoplasmic pH^{33,34}; such drops can be regulated³⁵ or result from internalization
514 of low-p*K*_a species such as short-chain fatty acids³⁶. Such changes could lead to
515 protonation of macromolecules involved in adsorption or changes in the proton
516 motive force³⁷. How these factors affect non-polycationic antibiotics such as
517 rifampin remains to be determined; neither of the ionizable functional groups of
518 rifampin (p*K*_as 1.7 and 7.9³⁸) nor erythromycin (p*K*_a 8.88³⁹) have p*K*_as in the pH
519 range achieved in our cultures (Fig. 2,S7b). Protonation changes in target
520 macromolecules could also lead to protection against antibiotics, although we
521 would expect a subsequent change in MIC, contrary to our findings (Fig. 1,5).
522 Intracellular acidification by the short-chain fatty acid propionate has been
523 proposed to lengthen lag phase in *Salmonella in vitro* and in the mouse gut⁴⁰,
524 consistent with our finding that lag time (Fig. 4) and intracellular pHluorin
525 fluorescence (Fig. S6a) are related.

526

527 Changes in intra- and extracellular pH have been shown to lead to
528 transcriptional responses that provide cross-protection against antibiotics⁴¹⁻⁴³,
529 suggesting that the killing retardation due to a pH increase in stationary phase
530 may result from a complex regulatory process. One major factor influencing the
531 *Lactobacillus-Acetobacter* interaction is that these organisms form a recurrent

532 community and may therefore have evolved to sense and benefit from each
533 other's presence. Further experiments are needed to uncover the molecular
534 mechanisms that link growth state and susceptibility to antibiotics in lactobacilli,
535 other non-model organisms, and microbial communities. In addition, although
536 we consistently observed related shifts in lag phase and tolerance (Fig. 3,5), it
537 remains to be established whether lag time and tolerance are causally linked or
538 coupled to some global variable, particularly given the opposite effects on
539 rifampin and erythromycin tolerance.

540

541 Previous work has shown that bacterial interactions can elicit changes in
542 antibiotic sensitivity by changing cellular physiology or interfering with
543 antibiotic action directly or indirectly⁹⁻¹¹. In principle, a myriad of intra- and
544 extra-cellular variables are subject to the composition and dynamics of the
545 ecosystems that bacteria inhabit, and microbial communities within mammalian
546 hosts can elicit changes in environmental variables both locally and globally.
547 Specifically, the microaerobic and anaerobic microenvironments of the human
548 and fly²⁴ gastrointestinal tracts enable the growth of short chain fatty acid
549 producers. Some of these short chain fatty acids, like butyrate, have been shown
550 to play an important role on host physiology and health⁴⁴. The consequences of
551 the accumulation of these short chain fatty acids and other small molecules on

552 microenvironments, as well as their effect on bacterial physiology and antibiotic
553 treatment efficacy *in vivo*, have yet to be systematically explored. Our results
554 emphasize the need to probe the action of antibiotics – as well as other drugs that
555 are thought not to target microbial growth⁴⁵ – in complex and varied conditions⁴⁶.
556 Furthermore, our findings highlight the utility of studying growth physiology in
557 co-cultures in the absence of antibiotics for uncovering novel mechanisms of
558 community-encoded protection against antibiotics.
559

560 **Online Methods**

561

562 *Fruit fly stocks and gut microbiome sequencing*

563 *Wolbachia*-free *Drosophila melanogaster* Canton-S (BL64349) flies were obtained
564 from the Bloomington *Drosophila* Stock Center, and were reared and maintained
565 as previously described²⁴. To determine the bacterial strains present in our flies,
566 we performed culture-independent 16S amplicon sequencing targeting the V4
567 region on an Illumina MiSeq. Individual flies were CO₂-anesthetized, surface-
568 sterilized by washing with 70% ethanol and sterile PBS six times each. Flies were
569 dissected under a stereo microscope and their guts were placed in 2-mL screw
570 cap microtubes containing 200 μ L of 0.1-mm sterile zirconia-silicate beads
571 (BioSpec Products 11079101z) and 350 μ L of sterile lysis buffer (10 mM Tris-HCl,
572 pH 8, 25 mM NaCl, 1 mM EDTA, 20 mg/mL lysozyme). Samples were
573 homogenized by bead beating at maximum speed (Mini-Beadbeater, BioSpec
574 Products) for 1 min. Proteinase K was added at 400 μ g/mL and samples were
575 incubated for 1 h at 37 °C. Samples were then centrifuged (3,000 \times g for 3 min) and
576 300 μ L of the nucleic acids-containing supernatant were transferred to 1.7-mL
577 microtubes. Genomic DNA from samples was cleaned up through a DNA Clean
578 & Concentrator-5 column (Zymo Research D4014). Using the protocol described
579 in Ref. ⁴⁷ for library preparation and sequencing, we sequenced the gut contents

580 of 18 individual flies, three flies each from six independent vials. Paired-end 250-
581 base pair sequencing generated >10,000 reads per sample. Reads were filtered
582 using PrinSeq as in Ref ⁴⁸. The reads were then clustered into operational
583 taxonomic units (OTUs) at 99% identity and assigned taxonomy using LOTUS⁴⁹
584 with the following parameters: [-threads 60 -refDB SLV -highmem 1 -id 0.99 -p
585 miseq -useBestBlastHitOnly 1 -derepMin 3:10,10:3 -simBasedTaxo 1 -CL 3].
586 Redundant strain identities were collapsed into single OTUs. Common reagent
587 contaminant strains were then removed⁵⁰. After filtering, only five unique species
588 were identified (Fig. 1a). We isolated these species in culture and verified the
589 taxonomic identity of our isolates using Sanger sequencing of the complete 16S
590 rRNA gene¹³. At 97% OTU clustering, only three species were found: *Acetobacter*
591 *sp.*, *Lactobacillus plantarum*, and *Lactobacillus brevis*. When less stringent FASTQ
592 quality filtering was used, trace amounts (~0.01%) of two mammalian gut strains
593 were identified: *Blautia sp.* and *Bacteroides sp.* Because these OTUs were
594 eliminated by more stringent quality filtering, we speculate that they may have
595 resulted from barcode bleed-through on the MiSeq flowcell.

596

597 *Bacterial growth and media*

598 Bacterial strains used in this study are listed in Supplementary Table 1. For
599 culturing, all strains were grown in MRS medium (Difco™ Lactobacilli MRS

600 Broth, BD 288110). Frozen stocks were streaked onto MRS agar plates (1.5% agar,
601 Difco™ agar, granulated, BD 214530) and single colonies were picked to start
602 cultures. MYPL medium was adapted from Ref. ⁵¹, with 1% (w/v) D-mannitol
603 (ACROS Organics AC125345000, Lot A0292699), 1% (w/v) yeast extract (Research
604 Products International Y20020, Lot 30553), 0.5% (w/v) peptone (Bacto™ peptone,
605 BD 211677 Lot 7065816), 1% (w/v) lactate (Lactic acid, Sigma L6661-100ML Lot
606 MKCC6092), and 0.1% (v/v) Tween® 80 (Polyoxyethylene(20)sorbitan
607 monooleate, ACROS Organics AC278632500 Lot A0375189). The medium was set
608 to pH 7 with NaOH (EMD Millipore SX0590, Lot B0484969043). All media were
609 filter-sterilized. Strains were grown at 30 °C with constant shaking.

610

611 To count CFUs in cultures, aliquots were diluted serially in PBS. For cultures
612 treated with high concentrations of antibiotics, cells were centrifuged for 1.5 min
613 at 8000 x g and resuspended in 1X PBS pH 7.4 (Gibco™ 70011044) after removing
614 the supernatants. PBS-diluted cultures were plated on MRS and MYPL because
615 lactobacilli grow faster than acetobacters on MRS and vice versa on MYPL.

616 Colony morphology and color enable differentiation of lactobacilli from
617 acetobacters.

618

619 *Conditioned media*

620 Conditioned media were obtained by centrifuging cultures at 4500 x g for 5 min
621 and filtering the supernatant with a 0.22- μ m polyethersulfone filter (Millex-GP
622 SLGP033RS) to remove cells. Conditioned media were acidified with HCl (Fisher
623 Chemical A144-500, Lot 166315) or basified with NaOH (EMD Millipore SX0590,
624 Lot B0484969043). Conditioned media were sterilized after adjusting pH with
625 0.22- μ m PES filters.

626

627 *MIC estimations*

628 To estimate the sensitivity of each species to various antibiotics, colonies were
629 inoculated into MRS and grown for 48 h at 30 °C with constant shaking. Cultures
630 were diluted to an OD of 0.001 for *Lp*, *Lb*, and *At*, and 0.01 for *Ap*. Diluted
631 cultures (195 μ L) were transferred to 96-well plates containing 5 μ L of antibiotics
632 at 40X the indicated concentration. Antibiotics used were ampicillin (ampicillin
633 sodium salt, MP Biomedicals 02194526, Lot R25707, stock at 100 mg/mL in milliQ
634 H₂O), streptomycin (streptomycin sulfate salt, Sigma S9137 Lot SLBN3225V,
635 stock at 50 mg/mL in milliQ H₂O), chloramphenicol (Calbiochem 220551, Lot
636 D00083225, stock at 50 mg/mL in ethanol), tetracycline (tetracycline
637 hydrochloride, MP Biomedicals 02103011, Lot 2297K, stock at 25 mg/mL in
638 dimethyl sulfoxide (DMSO)), erythromycin (Sigma E5389-1G, Lot WXBC4044V,
639 stock at 64 mg/mL in methanol), ciprofloxacin (Sigma-Aldrich 17850, Lot

640 116M4062CV, stock at 1.2 mg/mL in DMSO), trimethoprim (Alfa Aesar J63053-03,
641 Lot T16A009, stock at 2 mg/mL in DMSO), spectinomycin (spectinomycin
642 hydrochloride, Sigma-Aldrich PHR1426-500MG, Lot LRAA9208, stock at 50
643 mg/mL in milliQ H₂O), rifampin (Sigma R3501-5G, Lot SLBP9440V, stock at 50
644 mg/mL in DMSO), and vancomycin (vancomycin hydrochloride, Sigma-Aldrich
645 PHR1732-4X250MG, Lot LRAB3620, stock at 200 mg/mL in DMSO:H₂O 1:1).
646 Antibiotics were diluted serially in 2-fold increments into MRS. Cultures were
647 grown for 24 h at 30 °C with constant shaking and absorbance was measured in
648 an Epoch2 plate reader (BioTek Instruments) at 600 nm. The MIC was estimated
649 as the minimum concentration of antibiotic with absorbance within two standard
650 deviations of media controls.

651

652 For experiments in Supplementary Figure S2, colonies of *Lp* and *Ap* were
653 inoculated into MRS and grown for 48 h at 30 °C with constant shaking. The
654 saturated cultures were diluted to OD 0.02, mixed 1:1, and grown for 48 h at 30
655 °C with constant shaking. Then, the mono- and co-cultures were diluted to an
656 OD of 0.001 (final cell density $\sim 5 \times 10^5$ CFU/mL) and transferred to 96-well plates
657 containing 5 μ L of rifampin at 40X working concentration. Cultures were grown
658 for 24 h and MICs were estimated as described above. For Figures 1b-e, cultures
659 were serially diluted in 5-fold increments in PBS, and 3 μ L of the dilutions were

660 spotted onto MRS and MYPL rectangular plates using a semi-automated high-
661 throughput pipetting system (BenchSmart 96, Mettler Toledo). Plates were
662 incubated at 30 °C until colonies were visible for quantification of viability.

663

664 *Plate reader growth curves*

665 Cultures were grown from single colonies for 48 h in MRS at 30 °C with constant
666 shaking. Then, cultures were diluted to a final OD of 0.02 and 200 µL of the
667 dilutions were transferred to clear-bottom transparent 96-well plates. Plates were
668 sealed with transparent film pierced with a laser cutter to have ~0.5-mm holes to
669 allow aeration in each well. Absorbance was measured at 600 nm in an Epoch2
670 plate reader (BioTek Instruments). Plates were shaken between readings with
671 linear and orbital modes for 145 s each.

672

673 Growth rates and lag times were quantified using custom MATLAB (Mathworks,
674 R2008a) code. The natural logarithm of OD was smoothed with a mean filter
675 with window size of 5 timepoints for each condition over time, and the smoothed
676 data were used to calculate the instantaneous growth rate $d(\ln(\text{OD}))/dt$. The
677 smoothed $\ln(\text{OD})$ curve was fit to the Gompertz equation⁵² to determine lag time
678 and maximum growth rate.

679

680 *pH measurements*

681 Culture pH was measured using the dual-excitation ratiometric pH indicator
682 2',7-bis-(2-carboxyethyl)-5-(and-6)-carboxyfluorescein, mixed isomers (BCECF,
683 Invitrogen B1151, Lot 1831845), which has a pK_a of ~6.98. A stock solution of 1
684 mg/mL BCECF in DMSO (Fisher BioReagents BP231, Lot 165487) was diluted
685 1000-fold into MRS to a final concentration of 1 μ g/mL. Cells were grown in a
686 Synergy H1 plate reader (BioTek Instruments) following the procedure described
687 above. In addition to absorbance, fluorescence was measured every cycle using
688 monochromators at excitation (nm)/emission (nm) wavelength combinations
689 440/535 and 490/535. After subtracting the fluorescence of wells containing cells
690 without the indicator, the ratio of the signals excited at 440 nm and 490 nm was
691 used to calculate the culture pH using a calibration curve of MRS set to various
692 pH values.

693

694 Culture pH after 48 h of growth was directly measured with a pH meter
695 (sympHony, VWR) equipped with a pH combination electrode (Fisherbrand™
696 accumet™ 13-610-104A).

697

698 *Changes in pH during growth*

699 To change the pH of monocultures and co-cultures in stationary phase, we
700 obtained conditioned medium at 30 h or 40 h as described above and set the pH
701 to the desired values. We then centrifuged 2 mL of a replicate culture for 3 min at
702 8000 x g, removed the supernatant, and resuspended cells in 1 mL of the
703 corresponding medium to wash the cells. The suspension was centrifuged a
704 second time and the pellets were resuspended in 2 mL of the corresponding
705 medium.

706

707 *Time-lapse and fluorescence microscopy*

708 Cells were imaged on a Nikon Eclipse Ti-E inverted fluorescence microscope
709 with a 100× (NA 1.40) oil-immersion objective. Images were collected on a DU897
710 electron multiplying charged couple device camera (Andor) using μManager v.
711 1.4⁵³. Cells were maintained at 30 °C during imaging with an active-control
712 environmental chamber (Haison).

713

714 Cultures grown for 48 h were diluted 100-fold into PBS and 2 μL were spotted
715 onto a 1% (w/v) agarose MRS pad. After drying at room temperature, the pads
716 were covered with a cover slip, sealed with a mixture of equal portions of
717 Vaseline, lanolin, and paraffin, and transferred to the microscope. Images were
718 taken every 2 min using μManager v. 1.4.

719

720 To quantify the morphology of cells using fluorescent strains, co-cultures were
721 diluted 100-fold into PBS and 2 μ L were spotted onto a 1% (w/v) agarose PBS
722 pad. After drying, the pads were covered with a cover slip and transferred to the
723 microscope. Images were acquired at room temperature using μ Manager v. 1.4.

724

725 For Figure S6, saturated *Ap* monocultures were diluted 100- or 500-fold into PBS
726 and 2 μ L were spotted onto a 1% (w/v) agarose MRS pad containing 30 μ M
727 propidium iodide (from a 4.3-mM stock in water, BD, Cell Viability Kit 349483).

728 After drying, the pads were covered with a cover slip and transferred to the
729 microscope. Images were taken at 30 °C every 5 min using μ Manager v. 1.4.

730

731 The MATLAB image processing software *Morphometrics*⁵⁴ was used to segment
732 cells and to identify cell contours from phase-contrast images. Fluorescence
733 intensity per cell was calculated by averaging the fluorescence over the area of
734 the cell. A threshold for propidium-iodide labeling was defined that clearly
735 separated labeled cells from unlabeled cells (data not shown).

736

737 *Single-cell tracking and analysis*

738 Images were segmented and cells were tracked using the software *SuperSegger* v.
739 3⁵⁵. Further analysis of single-cell growth was performed using custom MATLAB
740 code. Cells with length >6 μm were removed from further analysis due to issues
741 with segmentation. Length traces were smoothed using a mean filter of window
742 size 5. Cells were classified as *Lp* or *Ap* if 90% of their traces were above (*Lp*) or
743 below (*Ap*) a \log_{10} (length-to-width ratio) of 0.375. Traces with more than 15
744 timepoints were used for further analysis. Elongation rates $d(\ln L)/dt$ were
745 calculated for each cell and the mean and standard error were computed for each
746 time point.

747

748 *Cloning and transformations*

749 To generate the fluorescently labeled *Ap* strain, the sfGFP coding sequence was
750 cloned into pCM62⁵⁶ under control of the *Escherichia coli* lac promoter. The sfGFP
751 coding sequence was amplified from pBAD-sfGFP using primers ZTG109 (5'
752 ggatttatgcATGAGCAAGGGCGAGGAG) and ZTG110 (5'-
753 gctttgtagcagccggatcgggcccggatctcgagTTACTTGTACAGCTCGTCCATG).
754 Gibson assembly⁵⁷ was used to insert the amplified sfGFP cassette into
755 BglII/XhoI-digested pCM62. This construct was delivered into *Ap* by conjugation
756 as previously described⁵⁸. *Escherichia coli* BW29427 was used as a donor strain
757 and maintained with 80 mg/mL 2,6-Diaminopimelic acid (Sigma Aldrich

758 33240)in potato agar mating plates⁵⁸. Transformed *Ap* was selected with 10
759 µg/mL tetracycline on yeast peptone glycerol agar plates⁵⁸.
760
761 To generate the *Lp* strain harboring pHluorin, the pHluorin coding sequence was
762 cloned into pCD256-mCherry⁵⁹ under the control of the strong p11 promoter²⁰.
763 The pHluorin coding sequence was amplified using primers ZFH064-pHluorin
764 (5'-ATTACAAGGAGATTTTACAT ATGAGTAAAGGAGAAGAAGACTTTTC) and
765 ZFH065-pHluorin (5'-
766 gtctcggacagcggttttGGATCCTTATTTGTATAGTTCATCCATG). Gibson
767 assembly⁵⁷ was used to insert the amplified pHluorin cassette into NdeI/BamHI-
768 digested pCD256-mCherry. The *Lp*-pHluorin strain was generated by
769 transforming wild type *Lp* as previously described⁶⁰.

770
771 Fluorescent strains were further grown in MRS with antibiotics (10 µg/mL
772 chloramphenicol (Calbiochem 220551, Lot D00083225) for *Lp*, tetracycline (10
773 µg/mL tetracycline hydrochloride, MP Biomedicals 02103011, Lot 2297K) for *Ap*).

774

775 *pHluorin measurements*

776 Cells were grown following the procedure described above. The *Lp* pHluorin
777 strain was grown in MRS containing 10 µg/mL chloramphenicol for the first 48 h

778 of growth. In addition to absorbance, fluorescence was measured every cycle
779 using monochromators at excitation (nm)/emission (nm) wavelength
780 combinations 405/509 and 475/509. Because the signal from excitation
781 wavelength 405 nm was undistinguishable from signal from medium (data not
782 shown), we also measured pHluorin signal at both excitation/emission
783 wavelength combinations for cells in PBS. Cultures (48-h-old, 250 μ L) were
784 centrifuged at 10,000 \times g for 1 min and resuspended in 1X PBS. Aliquots (200 μ L)
785 were transferred to a 96-well plate and fluorescence was measured using
786 monochromators at excitation (nm)/emission (nm) wavelength combinations
787 405/509 and 475/509 within 1 min of resuspension in a Synergy H1 plate reader
788 (BioTek Instruments).

789

790 *Lactate measurements*

791 Colonies of *Lp* and acetobacters were inoculated into 3 mL MRS and grown for
792 48 h at 30 °C with constant shaking. Saturated cultures were diluted to OD 0.02,
793 mixed 1:1, and grown at 30 °C with constant shaking. After mixing for 20 h and
794 48 h, a 700- μ L aliquot was transferred to a microcentrifuge tube and centrifuged
795 at 10,000 \times g for 4 min. Supernatant (600 μ L) was transferred to a new tube and
796 centrifuged at 10,000 \times g for 4 min. Supernatant (500 μ L) was transferred to a
797 new tube and kept on ice for not longer than 1 h, until lactate was measured.

798

799 L- and D-lactate concentrations were measured using the EnzyChrom™ L-
800 (BioAssay Systems ECLC-100, Lots BH06A30 and BI07A09) and D-lactate
801 (BioAssay Systems EDLC-100, Lots BH0420 and BI09A07) Assay Kits. Samples
802 were diluted 10- and 100-fold in water, and absorbance was measured according
803 to the manufacturer's instructions in a plate reader (Tecan M200). We also
804 included controls without lactate dehydrogenase to account for endogenous
805 activity in the supernatants.

806

807 *Ex vivo experiments*

808 We generated germ-free flies by sterilizing dechorionated embryos. Embryos
809 oviposited on grape juice-yeast medium (20% organic grape juice, 10% active dry
810 yeast, 5% glucose, 3% agar) were harvested and washed twice with 0.6% sodium
811 hypochlorite for 2.5 min each, once with 70% ethanol for 30 s, and three times in
812 sterile water for 10 s each. Eggs were transferred into flasks with sterile glucose-
813 yeast medium (10% glucose, 5% active dry yeast, 1.2% agar, 0.42% propionic
814 acid) and were maintained at 25 °C with 60% humidity and 12 h light/dark
815 cycles. Germ-free stocks of these flies were kept for several generations and were
816 regularly checked for sterility by plating flies onto MRS and YPD media.

817

818 To prepare flies for tolerance measurements, we took ~3-day-old germ-free flies
819 and transferred them to sterile vials with ~50 flies each. We added $\sim 5 \times 10^6$ CFU
820 of *Lp* onto the food and let the flies equilibrate with the bacteria for 3 days. The
821 day before the experiment, flies were transferred into a clean sterile vial.

822

823 To extract the midgut and crop, flies were washed with 70% ethanol and PBS six
824 times each. Flies were dissected under a stereo microscope in sterile PBS.

825 Dissected crops and midguts were pooled into 2 mL of sterile MRS with 200 μ L

826 0.5-mm diameter sterile zirconia-silicate beads (BioSpec Products 11079105).

827 Suspended organs were homogenized in a bead beater (Mini-Beadbeater,

828 BioSpec Products) at maximum speed for 1 min. The homogenate was diluted to

829 a cell density of $\sim 5 \times 10^5$ CFU/mL and was treated with 50 μ g/mL rifampin for 24

830 h.

831

832 *Statistical analyses*

833 To determine significance of differences, we performed pairwise Student's two-

834 sided *t*-tests throughout. To decrease Type I error, we performed Bonferroni

835 corrections for each experiment. Significant differences are denoted in the

836 figures: *: $P < 0.05/n$, **: $P < 0.01/n$, ***: $P < 0.001/n$, where *n* is the number of

837 comparisons.

838 **Acknowledgments**

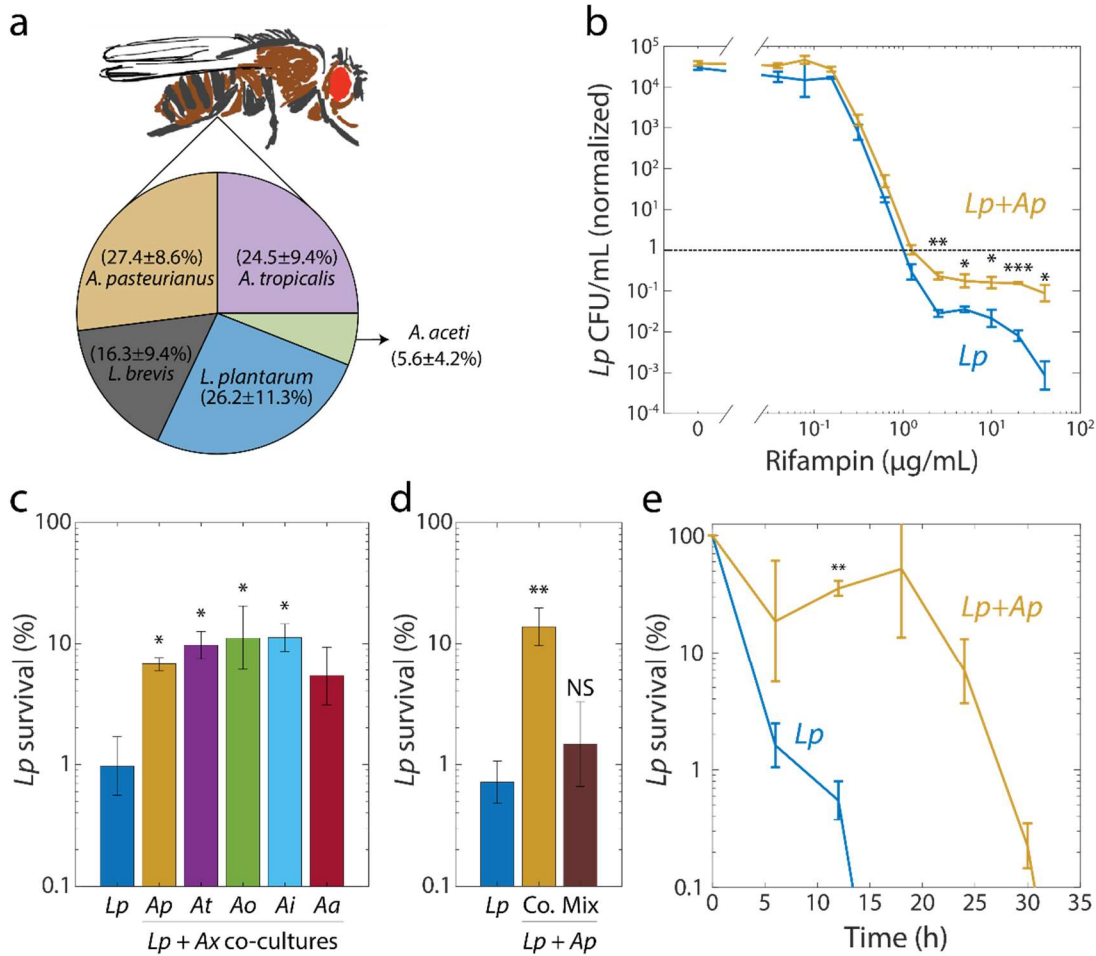
839 The authors thank Vivian Zhang for technical support, Elizabeth Skovran for
840 kindly providing the pCM62 plasmid for *Acetobacter* spp., and Kazunobu
841 Matsushita for providing the *A. tropicalis* SKU1100 control strain in the initial
842 conjugation experiments. We also thank the Huang and Ludington labs for
843 fruitful discussions. This work was supported by NIH Director's New Innovator
844 Awards DP2OD006466 (to K.C.H.), NSF CAREER Award MCB-1149328 (to
845 K.C.H.), the Allen Center for Systems Modeling of Infection (to K.C.H.), and NIH
846 Director's Early Independence Award DP5OD017851 (to W.B.L.). K.C.H. is a
847 Chan Zuckerberg Biohub Investigator. A.A.-D. is a Howard Hughes Medical
848 Institute International Student Research fellow and a Stanford Bio-X Bowes
849 fellow.

850

851 **Author Contributions**

852 A.A.-D., K.C.H., and W.B.L designed the research. A.A.-D. and T.T. performed *in*
853 *vitro* experiments. A.A.-D. and B.O. performed *ex vivo* experiments. B.O., Z.T.G.,
854 and Z.H. built fluorescent strains. A.A.-D. analyzed the data. A.A.-D., K.C.H.,
855 and W.B.L. wrote the paper. All authors reviewed the paper before submission.

856 **Figure Legends**



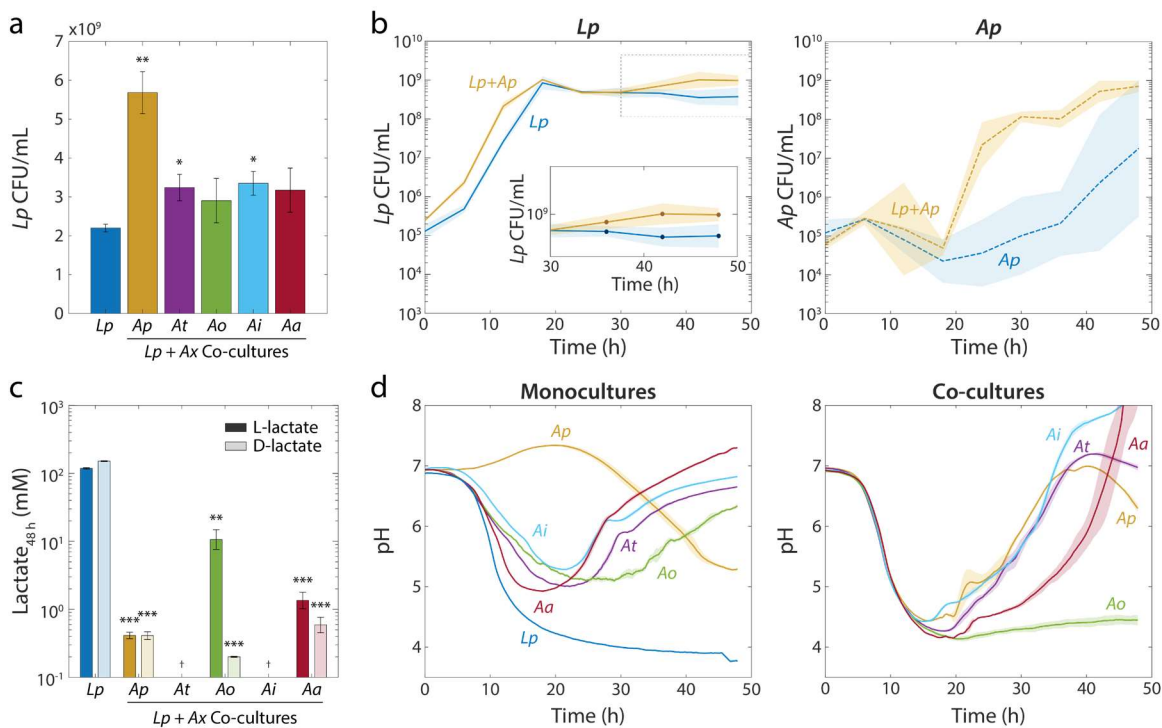
857

858 **Figure 1: Interspecies interactions within the fruit fly gut microbiome induce**
 859 **rifampin tolerance.**

860 a) Relative abundances of the dominant species in the *D. melanogaster* gut
 861 microbiome determined from 16S rRNA sequencing. Values are mean ±
 862 standard deviation (S.D.), *n*=18. Mean and S.D. were weighed by the total
 863 number of reads for each fly.

- 864 b) When grown with *Ap*, *Lp* survived after 24 h at rifampin concentrations above
865 the MIC. Viable cell plating counts of *Lp* after growth in rifampin for 24 h
866 normalized to the counts at the start of the experiment ($t=0$). Error bars are
867 standard deviation (S.D.) for each condition, $n=3$. P -values are from a
868 Student's two-sided t -test of the difference of the co-culture from the
869 monoculture (*: $P<4\times 10^{-3}$, **: $P<8\times 10^{-3}$, ***: $P<8\times 10^{-5}$).
- 870 c) Protection of *Lp* at supra-MIC concentrations of rifampin is elicited by all
871 acetobacters tested. Normalized CFUs of *Lp* grown in monoculture (*Lp*) or in
872 co-culture with *Ap*, *At*, *Ao*, *Ai*, and *Aa*, and then treated with 20 $\mu\text{g}/\text{mL}$
873 rifampin for 24 h. Error bars are S.D. for each condition, $n=3$. P -values are
874 from a Student's two-sided t -test of the difference from the monoculture (*:
875 $P<0.01$).
- 876 d) *Ap*-mediated survival of *Lp* at rifampin concentrations above the MIC is
877 history-dependent, requiring co-culturing before exposure as compared with
878 mixing. Normalized CFUs of *Lp* grown in monoculture, in co-culture with *Ap*
879 (Co.), or mixed with *Ap* without subsequent growth in the absence of
880 antibiotic (mix), and treated with 20 $\mu\text{g}/\text{mL}$ rifampin for 24 h. Error bars are
881 S.D. for each condition, $n=3$. P -values are from a Student's two-sided t -test of
882 the difference from the monoculture (**: $P<5\times 10^{-3}$, NS: not significant).

883 e) The time to killing of *Lp* under rifampin treatment is extended in the presence
884 of an *Acetobacter*. Normalized CFUs of *Lp* grown in monoculture and co-
885 cultured with *Ap*, and treated with 50 µg/mL rifampin. Error bars are S.D. for
886 each condition, $n=3$. P -values are from a Student's two-sided t -test of the
887 difference from the monoculture at the corresponding timepoint (**: $P<1\times 10^{-3}$).
888 Values off the graph were below the limit of detection of the assay
889



890

891 **Figure 2: *Lp* growth during stationary phase in *Acetobacter* co-cultures is**

892 **associated with an increase in pH and a decrease in lactate concentration.**

893 a) Co-culturing *Lp* with *Ap*, *At*, *Ai*, or *Aa* resulted in increased *Lp* cell density

894 after 48 h. Co-culturing with *Ao* did not significantly increase *Lp* cell

895 density by 48 h. Error bars are standard deviation (S.D.) for each

896 condition, $n=3$. P -values are from a Student's two-sided t -test of the

897 difference from the monoculture (*: $P<0.01$, **: $P<2\times 10^{-3}$).

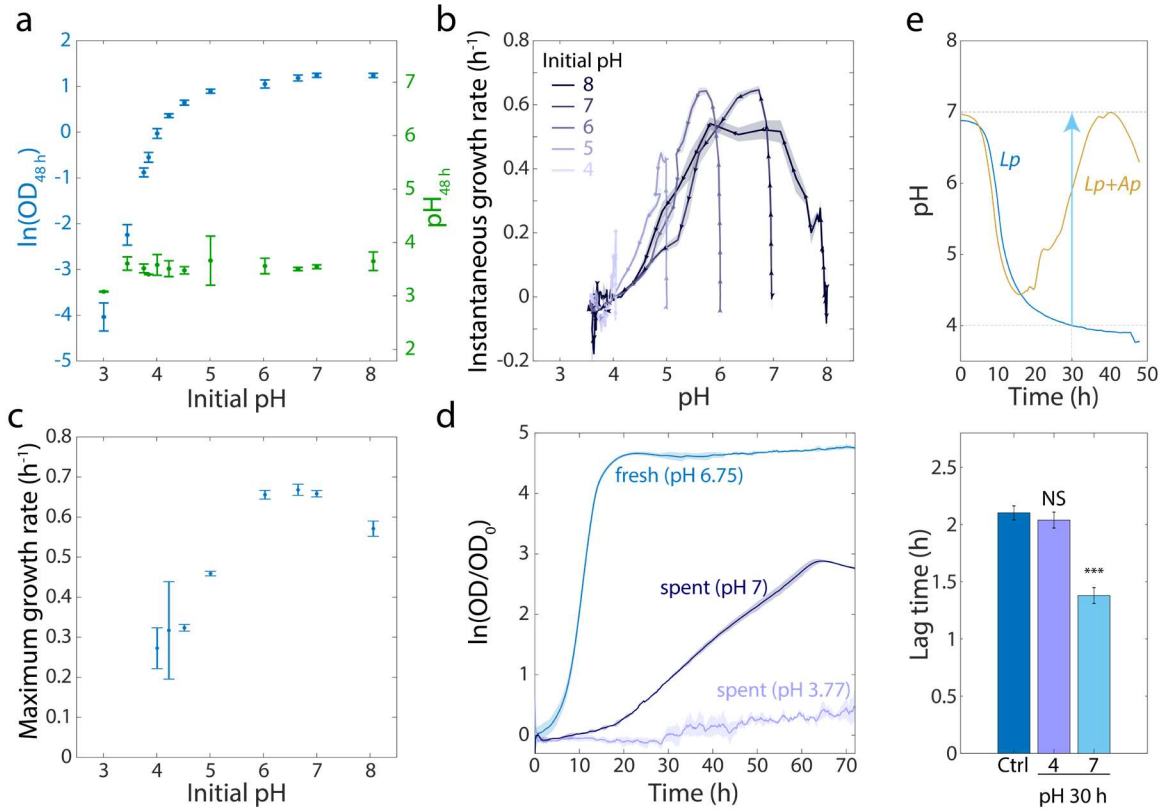
898 b) Co-culturing *Lp* with *Ap* resulted in higher *Lp* cell density in stationary

899 phase, as well as faster growth and shorter lag for *Ap*. Shaded regions

900 indicate S.D., $n=3$. Inset: zoom-in on region inside dashed box highlighting

901 increase in carrying capacity in co-culture.

- 902 c) L- and D-lactate were produced in *Lp* monocultures and consumed in co-
- 903 cultures. Lactate concentration was measured enzymatically from culture
- 904 supernatants at 48 h. Error bars are S.D. for each condition, $n=3$. *P*-values
- 905 are from a Student's two-sided *t*-test of the difference from the
- 906 monoculture (**: $P < 2 \times 10^{-3}$, ***: $P < 2 \times 10^{-4}$).
- 907 d) The increase in *Lp* cell density in stationary phase is associated with an
- 908 *Acetobacter*-dependent increase in pH early in stationary phase. pH was
- 909 measured with the pH-sensitive dye 2',7-bis-(2-carboxyethyl)-5-(and-6)-
- 910 carboxyfluorescein over time (Methods). Shaded regions indicate S.D.,
- 911 $n=3$.

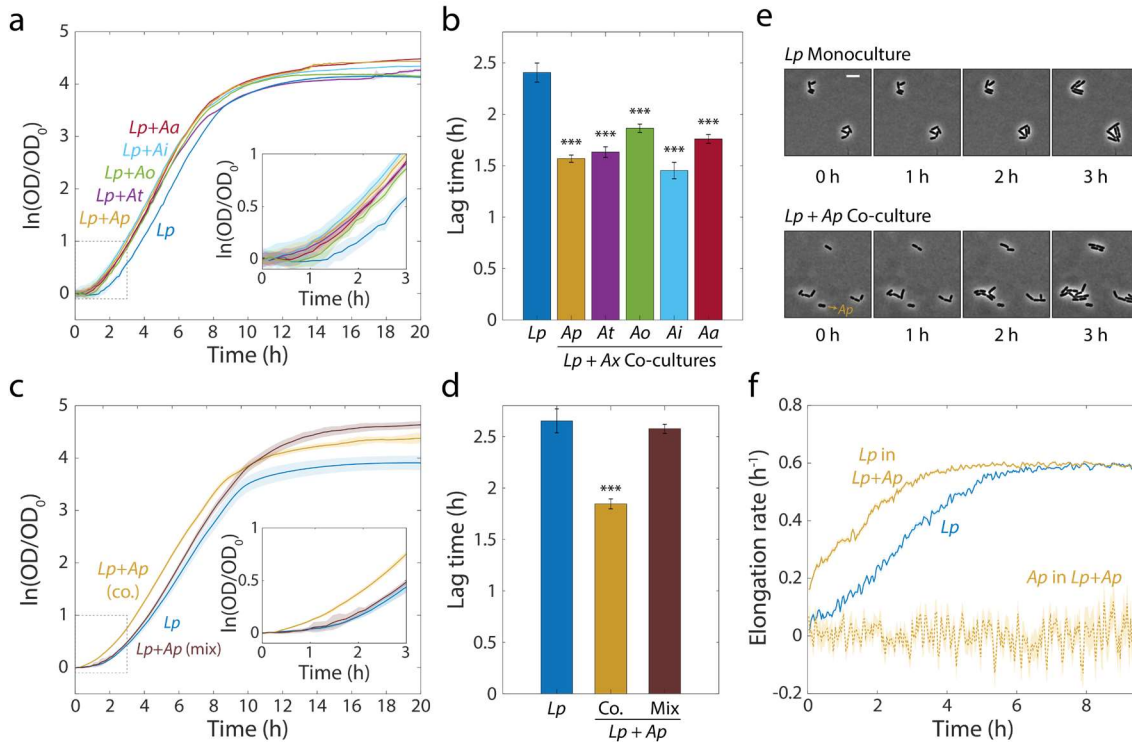


912

913 **Figure 3: An increase in extracellular pH in stationary phase releases growth**
914 **inhibition in *Lp* monocultures and shortens lag phase.**

915 a) *Lp* growth is inhibited by low pH. Logarithm of OD (blue) and pH
916 measured using BCECF (green) after 48 h of growth in MRS at various
917 starting pH values. Error bars are standard deviation (S.D.), $n=4$.
918 b) Instantaneous growth rate in MRS is strongly linked to pH. Each curve
919 was initialized at a different starting pH and represents 48 h of growth.
920 Arrowheads indicate direction of time. Shaded regions are S.D., $n=4$.
921 c) Maximal growth rate in MRS increases with increasing initial pH. Error
922 bars are S.D., $n=4$.

- 923 d) Increasing the pH of a saturated, spent *Lp* culture from 3.77 to 7 allows
924 growth, although not as much as fresh MRS. Error bars are S.D., $n = 3$.
- 925 e) Increasing the pH of an *Lp* monoculture at $t = 30$ h from 4 to 7 to mimic the
926 pH increase in *Lp-Ap* co-culture (top) leads to a shorter lag phase (bottom).
927 Lag time was calculated by fitting growth curves to the Gompertz
928 equation. Error bars are S.D., $n=3$. P -values are from a Student's two-sided
929 t -test of the difference from the control (***: $P < 5 \times 10^{-4}$, NS: not significant).
930



931

932 **Figure 4: Co-cultures of *Lp* and acetobacters undergo shorter lag phases.**

933 a) Calculating the logarithm of OD normalized by OD at $t=0$ reveals that co-

934 cultures of *Lp* and various acetobacters (A_x) experience more rapid

935 transitions from stationary phase to exponential growth than

936 monocultures of *Lp*. Shaded regions indicate standard deviation (S.D.),

937 $n=5$. Inset: zoom-in of region inside dashed box highlighting lag

938 differences.

939 b) Co-culture lag times are significantly shorter than *Lp* monoculture lag

940 times. Lag times were obtained by fitting the growth curves in (a) to the

941 Gompertz equation. Error bars are S.D. for each condition, $n=5$. P -values

942 are from a Student's two-sided t -test of the difference from the
943 monoculture (***: $P < 2 \times 10^{-4}$).

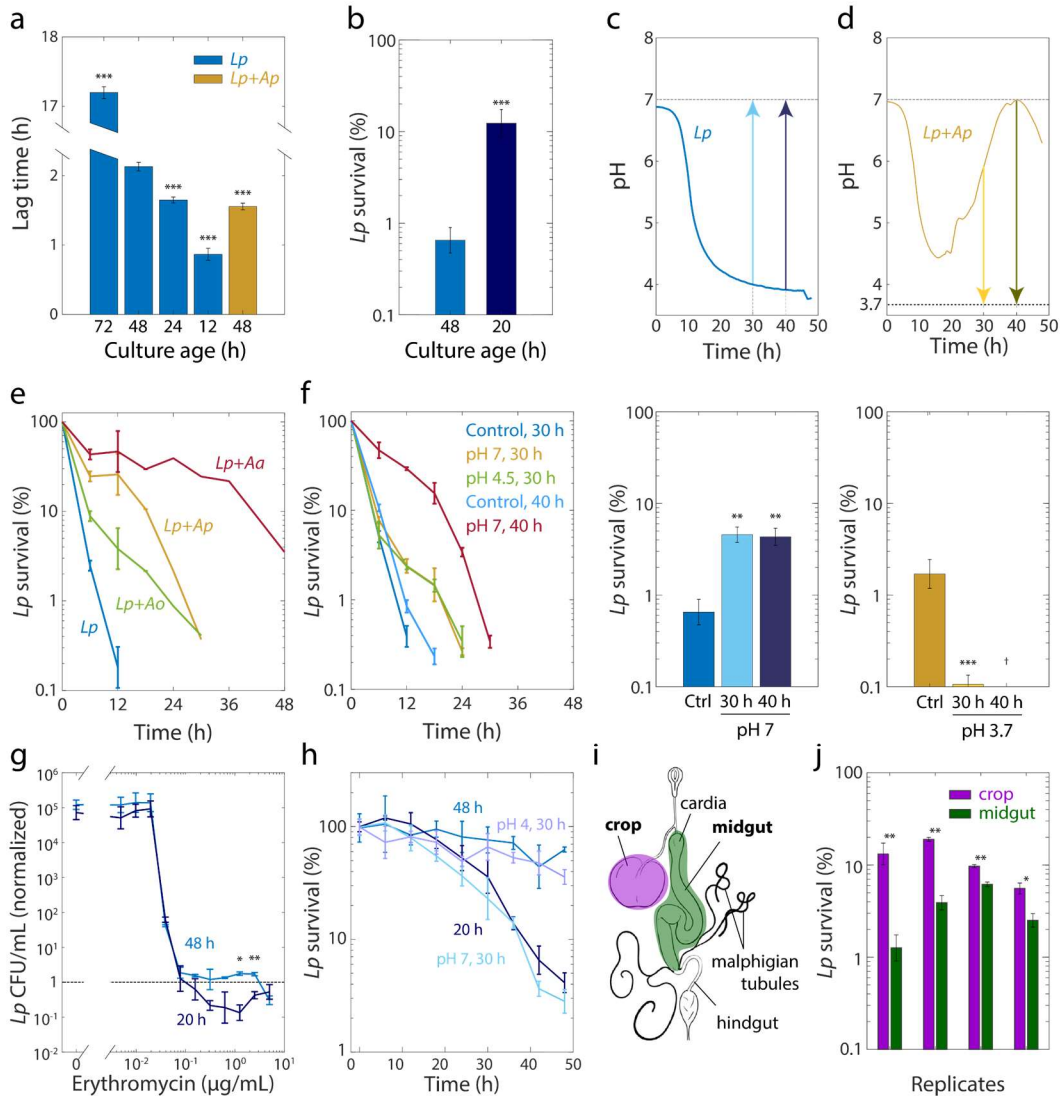
944 c) Mixing Lp monocultures with Ap monocultures (Mix) yields growth
945 curves with a similar lag phase than those of Lp monocultures. Shaded
946 regions indicate S.D., $n=5$. Inset: zoom-in on region inside dashed box
947 highlighting lag differences.

948 d) Mixed Lp - Ap cultures do not experience significantly shorter lag times
949 than Lp monocultures. Lag times were obtained by fitting the curves in (c)
950 to the Gompertz equation. Error bars are S.D. for each condition, $n=5$. P -
951 values are from a Student's two-sided t -test of the difference from the
952 monoculture (***: $P < 5 \times 10^{-4}$).

953 e) Single-cell microscopy demonstrates that a decrease in the duration of lag
954 phase of Lp was responsible for the lag-time decrease in co-culture.
955 Representative phase microscopy images of Lp in monoculture and co-
956 cultured with Ap on an MRS agar pad. The only Ap cell visible in these
957 images is indicated with an arrow. Size bar = 5 μm .

958 f) The instantaneous elongation rate of single Lp cells increases faster in co-
959 culture than in monoculture. Phase-contrast images were segmented and
960 cells were classified as Lp or Ap based on their aspect ratio. Lines are the
961 mean and shaded regions are the standard error for an Lp monoculture

962 $(n_{Lp,0h} = 465, n_{Lp,9.5h} = 27,503)$ or a co-culture with *Ap* ($n_{Lp,0h} = 448, n_{Lp,9.5h} =$
963 $58,087, n_{Ap,0h} = 47, n_{Ap,9.5h} = 146$).



964

965 **Figure 5: Tolerance to rifampin is modulated by pH.**

966 a) The duration of lag phase of bulk cultures of *Lp* depends on the time spent
 967 in stationary phase. *Lp* monocultures grown for various times from
 968 OD=0.02, and co-cultures with *Ap*, were diluted into fresh medium. Lag
 969 time was calculated by fitting growth curves to the Gompertz equation.
 970 Error bars are standard deviation (S.D.), $n=12$. P -values are from a

971 Student's two-sided *t*-test of the difference with respect to the 48 h culture

972 ($***P < 2.5 \times 10^{-4}$).

973 b) Culturing *Lp* as a monoculture for a shorter time leads to higher cell

974 survival. Viable cell plating counts of *Lp* after growth in 20 $\mu\text{g/mL}$

975 rifampin for 24 h normalized to the counts at the start of the experiment

976 ($t=0$). Error bars are S.D. for each condition, $n=3$. *P*-values are from a

977 Student's two-sided *t*-test of the difference between the cultures ($***$:

978 $P < 1 \times 10^{-3}$).

979 c) Neutralization of pH in stationary phase in *Lp* monocultures is sufficient

980 to induce tolerance. Increasing the pH of an *Lp* monoculture at $t = 30$ h or t

981 $= 40$ h to 7 to mimic the pH increase in co-cultures of *Lp* with acetobacters

982 (upper panel) increased cell survival after treatment with 20 $\mu\text{g/mL}$

983 rifampin for 24 h (lower panel). A 48-h-old culture with no changes in pH

984 was used as a control (Ctrl.). Error bars are S.D. for each condition, $n=3$. *P*-

985 values are from a Student's two-sided *t*-test of the difference between the

986 cultures ($**$: $P < 5 \times 10^{-3}$).

987 d) Acidification of *Lp* co-cultures with *Ap* during the exponential-to-

988 stationary phase transition or in late stationary phase sensitizes *Lp* to

989 rifampin. Decreasing the pH of an *Lp* co-culture with *Ap* at $t = 30$ h or $t =$

990 40 h to 3.7 to mimic the pH of an *Lp* monoculture (upper panel) increased

991 survival after treatment with 20 $\mu\text{g}/\text{mL}$ rifampin for 24 h (lower panel).

992 Error bars are S.D. for each condition, $n=3$. P -values are from a Student's

993 two-sided t -test of the difference between the cultures (***: $P<5\times 10^{-4}$).

994 [†]Values below the limit of detection.

995 e) The dynamics of killing in *Lp* co-culture with acetobacters differs

996 quantitatively according to species and from *Lp* monoculture (blue),

997 indicating that the acetobacters induce rifampin tolerance to different

998 degrees. Normalized CFU/mL of *Lp* in monoculture and in co-culture with

999 acetobacters, and treated with 50 $\mu\text{g}/\text{mL}$ rifampin. Error bars are S.D. for

1000 each condition, $n=3$.

1001 f) The timing of the pH change in *Acetobacter* co-culture predicts the extent

1002 of protection against 50 $\mu\text{g}/\text{mL}$ rifampin. Neutralization of pH in *Lp*

1003 monocultures at 40 h of growth (to mimic *Lp+Aa* co-cultures) elicits longer

1004 protection against rifampin than neutralization at 30 h. A small increase in

1005 pH (from 3.85 to 4.5) at 30 h (to mimic *Lp+Ao* co-cultures) provides

1006 protection comparable to complete neutralization. Error bars are S.D. for

1007 each condition, $n=3$.

1008 g) *Lp* survival to erythromycin is ~10 times higher after 24 h of treatment

1009 with erythromycin at supraMIC concentrations on 48-h-old monocultures

1010 (48 h) of *Lp* than on 20-h-old *Lp* monocultures (20 h). Viable cell plating

1011 counts of *Lp* after growth in erythromycin for 24 h normalized to cell
1012 counts at the start of the experiment ($t=0$). Error bars are S.D., $n = 3$. *P*-
1013 values are from a Student's two-sided *t*-test of the difference between the
1014 two samples at a given time point (*: $P < 4 \times 10^{-3}$, **: $P < 8 \times 10^{-4}$).

1015 h) Shifting the pH of an *Lp* monoculture at 30 h to 4 or 7, followed by 18 h of
1016 growth before treatment with 2 $\mu\text{g}/\text{mL}$ erythromycin, mimics the survival
1017 dynamics of a 48-h-old or 20-h-old culture in stationary phase,
1018 respectively. Normalized CFU/mL of *Lp* monocultures. Error bars are S.D.
1019 for each condition, $n=3$.

1020 i) Schematic of the fruit fly intestinal tract, a ~5 mm-long tube consisting of
1021 the foregut, midgut, and hindgut. The crop is an accessory fermentative
1022 organ within the foregut.

1023 j) Survival of *Lp* is significantly higher in bulk cultures resuspended from
1024 the crop than in cultures resuspended from the midgut. Female, ~7-day-
1025 old, germ-free flies were colonized with *Lp* and left for three days in sterile
1026 food to reach equilibrium, before the crop was dissected from the midgut
1027 (Methods). After homogenization of pools of crops and midguts, the
1028 cultures were exposed to 50 $\mu\text{g}/\text{mL}$ rifampin for 24 h and viable cells were
1029 counted via CFU. Error bars are S.D. of the technical replicates for each
1030 biological replicate, $n=3$ in each biological replicate. *P*-values are from a

1031 Student's two-sided t -test of the difference between the two samples (*:

1032 $P < 1.25 \times 10^{-2}$, **: $P < 2.5 \times 10^{-3}$).

1033 **References**

1034

- 1035 1 Thulin, E., Sundqvist, M. & Andersson, D. I. Amdinocillin (Mecillinam)
1036 resistance mutations in clinical isolates and laboratory-selected mutants of
1037 *Escherichia coli*. *Antimicrob Agents Chemother* **59**, 1718-1727,
1038 doi:10.1128/AAC.04819-14 (2015).
- 1039 2 Dethlefsen, L., Huse, S., Sogin, M. L. & Relman, D. A. The pervasive
1040 effects of an antibiotic on the human gut microbiota, as revealed by deep
1041 16S rRNA sequencing. *PLoS Biol* **6**, e280, doi:10.1371/journal.pbio.0060280
1042 (2008).
- 1043 3 Jernberg, C., Lofmark, S., Edlund, C. & Jansson, J. K. Long-term ecological
1044 impacts of antibiotic administration on the human intestinal microbiota.
1045 *ISME J* **1**, 56-66, doi:10.1038/ismej.2007.3 (2007).
- 1046 4 Santajit, S. & Indrawattana, N. Mechanisms of Antimicrobial Resistance in
1047 ESKAPE Pathogens. *Biomed Res Int* **2016**, 2475067,
1048 doi:10.1155/2016/2475067 (2016).
- 1049 5 Brauner, A., Fridman, O., Gefen, O. & Balaban, N. Q. Distinguishing
1050 between resistance, tolerance and persistence to antibiotic treatment. *Nat*
1051 *Rev Microbiol* **14**, 320-330, doi:10.1038/nrmicro.2016.34 (2016).
- 1052 6 Nicoloff, H. & Andersson, D. I. Indirect resistance to several classes of
1053 antibiotics in cocultures with resistant bacteria expressing antibiotic-
1054 modifying or -degrading enzymes. *J Antimicrob Chemother* **71**, 100-110,
1055 doi:10.1093/jac/dkv312 (2016).
- 1056 7 Sanchez-Vizueté, P., Orgaz, B., Aymerich, S., Le Coq, D. & Briandet, R.
1057 Pathogens protection against the action of disinfectants in multispecies
1058 biofilms. *Front Microbiol* **6**, 705, doi:10.3389/fmicb.2015.00705 (2015).
- 1059 8 de Vos, M. G. J., Zagorski, M., McNally, A. & Bollenbach, T. Interaction
1060 networks, ecological stability, and collective antibiotic tolerance in
1061 polymicrobial infections. *Proc Natl Acad Sci U S A* **114**, 10666-10671,
1062 doi:10.1073/pnas.1713372114 (2017).
- 1063 9 Adamowicz, E. M., Flynn, J., Hunter, R. C. & Harcombe, W. R. Cross-
1064 feeding modulates antibiotic tolerance in bacterial communities. *ISME J*,
1065 doi:10.1038/s41396-018-0212-z (2018).
- 1066 10 Radlinski, L. *et al.* *Pseudomonas aeruginosa* exoproducts determine
1067 antibiotic efficacy against *Staphylococcus aureus*. *PLoS Biol* **15**, e2003981,
1068 doi:10.1371/journal.pbio.2003981 (2017).
- 1069 11 Sorg, R. A. *et al.* Collective Resistance in Microbial Communities by
1070 Intracellular Antibiotic Deactivation. *PLoS Biol* **14**, e2000631,
1071 doi:10.1371/journal.pbio.2000631 (2016).

- 1072 12 Ratzke, C. & Gore, J. Modifying and reacting to the environmental pH can
1073 drive bacterial interactions. *PLoS Biol* **16**, e2004248,
1074 doi:10.1371/journal.pbio.2004248 (2018).
- 1075 13 Gould, A. L. *et al.* Microbiome interactions shape host fitness. *Proc Natl*
1076 *Acad Sci U S A*, doi:10.1073/pnas.1809349115 (2018).
- 1077 14 Wong, C. N., Ng, P. & Douglas, A. E. Low-diversity bacterial community
1078 in the gut of the fruitfly *Drosophila melanogaster*. *Environ Microbiol* **13**,
1079 1889-1900, doi:10.1111/j.1462-2920.2011.02511.x (2011).
- 1080 15 Makarova, K. *et al.* Comparative genomics of the lactic acid bacteria. *Proc*
1081 *Natl Acad Sci U S A* **103**, 15611-15616, doi:10.1073/pnas.0607117103 (2006).
- 1082 16 Yamada, Y., Hoshino, K. & Ishikawa, T. The phylogeny of acetic acid
1083 bacteria based on the partial sequences of 16S ribosomal RNA: the
1084 elevation of the subgenus *Gluconoacetobacter* to the generic level. *Biosci*
1085 *Biotechnol Biochem* **61**, 1244-1251, doi:10.1271/bbb.61.1244 (1997).
- 1086 17 Walsh, C. & Wencewicz, T. A. *Antibiotics : challenges, mechanisms,*
1087 *opportunities.* (ASM Press, 2016).
- 1088 18 James-Kracke, M. R. Quick and accurate method to convert BCECF
1089 fluorescence to pH_i: calibration in three different types of cell
1090 preparations. *J Cell Physiol* **151**, 596-603, doi:10.1002/jcp.1041510320 (1992).
- 1091 19 Martinez, K. A., 2nd *et al.* Cytoplasmic pH response to acid stress in
1092 individual cells of *Escherichia coli* and *Bacillus subtilis* observed by
1093 fluorescence ratio imaging microscopy. *Applied and environmental*
1094 *microbiology* **78**, 3706-3714, doi:10.1128/AEM.00354-12 (2012).
- 1095 20 Rud, I., Jensen, P. R., Naterstad, K. & Axelsson, L. A synthetic promoter
1096 library for constitutive gene expression in *Lactobacillus plantarum*.
1097 *Microbiology* **152**, 1011-1019, doi:10.1099/mic.0.28599-0 (2006).
- 1098 21 Levin-Reisman, I. *et al.* Automated imaging with ScanLag reveals
1099 previously undetectable bacterial growth phenotypes. *Nat Methods* **7**, 737-
1100 739, doi:10.1038/nmeth.1485 (2010).
- 1101 22 Buchon, N. *et al.* Morphological and molecular characterization of adult
1102 midgut compartmentalization in *Drosophila*. *Cell Rep* **3**, 1725-1738,
1103 doi:10.1016/j.celrep.2013.04.001 (2013).
- 1104 23 Strand, M. & Micchelli, C. A. Quiescent gastric stem cells maintain the
1105 adult *Drosophila* stomach. *Proc Natl Acad Sci U S A* **108**, 17696-17701,
1106 doi:10.1073/pnas.1109794108 (2011).
- 1107 24 Obadia, B. *et al.* Probabilistic Invasion Underlies Natural Gut Microbiome
1108 Stability. *Curr Biol* **27**, 1999-2006 e1998, doi:10.1016/j.cub.2017.05.034
1109 (2017).
- 1110 25 Boris, S. & Barbes, C. Role played by lactobacilli in controlling the
1111 population of vaginal pathogens. *Microbes Infect* **2**, 543-546 (2000).

- 1112 26 Brauner, A., Shores, N., Fridman, O. & Balaban, N. Q. An Experimental
1113 Framework for Quantifying Bacterial Tolerance. *Biophys J* **112**, 2664-2671,
1114 doi:10.1016/j.bpj.2017.05.014 (2017).
- 1115 27 Fridman, O., Goldberg, A., Ronin, I., Shores, N. & Balaban, N. Q.
1116 Optimization of lag time underlies antibiotic tolerance in evolved bacterial
1117 populations. *Nature* **513**, 418-421, doi:10.1038/nature13469 (2014).
- 1118 28 Levin-Reisman, I. *et al.* Antibiotic tolerance facilitates the evolution of
1119 resistance. *Science* **355**, 826-830, doi:10.1126/science.aaj2191 (2017).
- 1120 29 Rotem, E. *et al.* Regulation of phenotypic variability by a threshold-based
1121 mechanism underlies bacterial persistence. *Proc Natl Acad Sci U S A* **107**,
1122 12541-12546, doi:10.1073/pnas.1004333107 (2010).
- 1123 30 Mouery, K., Rader, B. A., Gaynor, E. C. & Guillemin, K. The stringent
1124 response is required for *Helicobacter pylori* survival of stationary phase,
1125 exposure to acid, and aerobic shock. *J Bacteriol* **188**, 5494-5500,
1126 doi:10.1128/JB.00366-06 (2006).
- 1127 31 Abranches, J. *et al.* The molecular alarmone (p)ppGpp mediates stress
1128 responses, vancomycin tolerance, and virulence in *Enterococcus faecalis*. *J*
1129 *Bacteriol* **191**, 2248-2256, doi:10.1128/JB.01726-08 (2009).
- 1130 32 Peters, K. *et al.* The Redundancy of Peptidoglycan Carboxypeptidases
1131 Ensures Robust Cell Shape Maintenance in *Escherichia coli*. *MBio* **7**,
1132 doi:10.1128/mBio.00819-16 (2016).
- 1133 33 Choi, J. & Groisman, E. A. Acidic pH sensing in the bacterial cytoplasm is
1134 required for *Salmonella* virulence. *Mol Microbiol* **101**, 1024-1038,
1135 doi:10.1111/mmi.13439 (2016).
- 1136 34 Olsen, K. N. *et al.* Noninvasive measurement of bacterial intracellular pH
1137 on a single-cell level with green fluorescent protein and fluorescence ratio
1138 imaging microscopy. *Applied and environmental microbiology* **68**, 4145-4147
1139 (2002).
- 1140 35 Chakraborty, S., Mizusaki, H. & Kenney, L. J. A FRET-based DNA
1141 biosensor tracks OmpR-dependent acidification of *Salmonella* during
1142 macrophage infection. *PLoS Biol* **13**, e1002116,
1143 doi:10.1371/journal.pbio.1002116 (2015).
- 1144 36 Ricke, S. C. Perspectives on the use of organic acids and short chain fatty
1145 acids as antimicrobials. *Poult Sci* **82**, 632-639, doi:10.1093/ps/82.4.632
1146 (2003).
- 1147 37 Krulwich, T. A., Sachs, G. & Padan, E. Molecular aspects of bacterial pH
1148 sensing and homeostasis. *Nat Rev Microbiol* **9**, 330-343,
1149 doi:10.1038/nrmicro2549 (2011).

- 1150 38 Maggi, N., Pasqualucci, C. R., Ballotta, R. & Sensi, P. Rifampicin: a new
1151 orally active rifamycin. *Chemotherapy* **11**, 285-292, doi:10.1159/000220462
1152 (1966).
- 1153 39 McFarland, J. W. *et al.* Quantitative structure-activity relationships among
1154 macrolide antibacterial agents: in vitro and in vivo potency against
1155 *Pasteurella multocida*. *J Med Chem* **40**, 1340-1346, doi:10.1021/jm960436i
1156 (1997).
- 1157 40 Jacobson, A. *et al.* A Gut Commensal-Produced Metabolite Mediates
1158 Colonization Resistance to Salmonella Infection. *Cell Host Microbe* **24**, 296-
1159 307 e297, doi:10.1016/j.chom.2018.07.002 (2018).
- 1160 41 Komora, N., Bruschi, C., Magalhaes, R., Ferreira, V. & Teixeira, P. Survival
1161 of *Listeria monocytogenes* with different antibiotic resistance patterns to
1162 food-associated stresses. *Int J Food Microbiol* **245**, 79-87,
1163 doi:10.1016/j.ijfoodmicro.2017.01.013 (2017).
- 1164 42 McMahan, M. A., Xu, J., Moore, J. E., Blair, I. S. & McDowell, D. A.
1165 Environmental stress and antibiotic resistance in food-related pathogens.
1166 *Applied and environmental microbiology* **73**, 211-217, doi:10.1128/AEM.00578-
1167 06 (2007).
- 1168 43 O'Sullivan, E. & Condon, S. Intracellular pH is a major factor in the
1169 induction of tolerance to acid and other stresses in *Lactococcus lactis*.
1170 *Applied and environmental microbiology* **63**, 4210-4215 (1997).
- 1171 44 Nicholson, J. K. *et al.* Host-gut microbiota metabolic interactions. *Science*
1172 **336**, 1262-1267, doi:10.1126/science.1223813 (2012).
- 1173 45 Maier, L. *et al.* Extensive impact of non-antibiotic drugs on human gut
1174 bacteria. *Nature* **555**, 623-628, doi:10.1038/nature25979 (2018).
- 1175 46 Beppler, C. *et al.* When more is less: Emergent suppressive interactions in
1176 three-drug combinations. *BMC Microbiol* **17**, 107, doi:10.1186/s12866-017-
1177 1017-3 (2017).
- 1178 47 Fadrosch, D. W. *et al.* An improved dual-indexing approach for
1179 multiplexed 16S rRNA gene sequencing on the Illumina MiSeq platform.
1180 *Microbiome* **2**, 6, doi:10.1186/2049-2618-2-6 (2014).
- 1181 48 Koch, M. A. *et al.* Maternal IgG and IgA Antibodies Dampen Mucosal T
1182 Helper Cell Responses in Early Life. *Cell* **165**, 827-841,
1183 doi:10.1016/j.cell.2016.04.055 (2016).
- 1184 49 Hildebrand, F., Tadeo, R., Voigt, A. Y., Bork, P. & Raes, J. LotuS: an
1185 efficient and user-friendly OTU processing pipeline. *Microbiome* **2**, 30,
1186 doi:10.1186/2049-2618-2-30 (2014).
- 1187 50 Salter, S. J. *et al.* Reagent and laboratory contamination can critically
1188 impact sequence-based microbiome analyses. *BMC Biol* **12**, 87,
1189 doi:10.1186/s12915-014-0087-z (2014).

- 1190 51 Moens, F., Lefeber, T. & De Vuyst, L. Oxidation of metabolites highlights
1191 the microbial interactions and role of *Acetobacter pasteurianus* during
1192 cocoa bean fermentation. *Applied and environmental microbiology* **80**, 1848-
1193 1857, doi:10.1128/AEM.03344-13 (2014).
- 1194 52 Zwietering, M. H., Jongenburger, I., Rombouts, F. M. & van 't Riet, K.
1195 Modeling of the bacterial growth curve. *Applied and environmental*
1196 *microbiology* **56**, 1875-1881 (1990).
- 1197 53 Edelstein, A., Amodaj, N., Hoover, K., Vale, R. & Stuurman, N. *Computer*
1198 *Control of Microscopes Using μ Manager*. (John Wiley & Sons, Inc., 2010).
- 1199 54 Ursell, T. *et al.* Rapid, precise quantification of bacterial cellular
1200 dimensions across a genomic-scale knockout library. *BMC biology* **15**, 17
1201 (2017).
- 1202 55 Stylianidou, S., Brennan, C., Nissen, S. B., Kuwada, N. J. & Wiggins, P. A.
1203 SuperSegger: robust image segmentation, analysis and lineage tracking of
1204 bacterial cells. *Mol Microbiol* **102**, 690-700, doi:10.1111/mmi.13486 (2016).
- 1205 56 Marx, C. J. & Lidstrom, M. E. Development of improved versatile broad-
1206 host-range vectors for use in methylotrophs and other Gram-negative
1207 bacteria. *Microbiology* **147**, 2065-2075, doi:10.1099/00221287-147-8-2065
1208 (2001).
- 1209 57 Gibson, D. G. *et al.* Enzymatic assembly of DNA molecules up to several
1210 hundred kilobases. *Nature Methods* **6**, 343-345, doi:10.1038/nmeth.1318
1211 (2009).
- 1212 58 Deeraksa, A. *et al.* Characterization and spontaneous mutation of a novel
1213 gene, *polE*, involved in pellicle formation in *Acetobacter tropicalis*
1214 SKU1100. *Microbiology* **151**, 4111-4120, doi:10.1099/mic.0.28350-0 (2005).
- 1215 59 Spath, K., Heinl, S., Egger, E. & Grabherr, R. *Lactobacillus plantarum* and
1216 *Lactobacillus buchneri* as expression systems: evaluation of different origins
1217 of replication for the design of suitable shuttle vectors. *Mol Biotechnol* **52**,
1218 40-48 (2012).
- 1219 60 Spath, K., Heinl, S. & Grabherr, R. "Direct cloning in *Lactobacillus*
1220 *plantarum*: electroporation with non-methylated plasmid DNA enhances
1221 transformation efficiency and makes shuttle vectors obsolete". *Microb Cell*
1222 *Fact* **11**, 141, doi:10.1186/1475-2859-11-141 (2012).
- 1223